ISTANBUL TECHNICAL UNIVERSITY ★ GRADUATE SCHOOL

DESIGN OF AN ORIGAMI STRUCTURED DEPLOYABLE S-BAND HELICAL ANTENNA FOR 6U CUBESATS

M.Sc. THESIS

Rümeysa ÜSTÜNCAN

Department of Defense Technologies

Defense Technologies Programme

JUNE 2025

ISTANBUL TECHNICAL UNIVERSITY ★ GRADUATE SCHOOL

DESIGN OF AN ORIGAMI STRUCTURED DEPLOYABLE S-BAND HELICAL ANTENNA FOR 6U CUBESATS

M.Sc. THESIS

Rümeysa ÜSTÜNCAN
(514221036)

Department of Defense Technologies

Defense Technologies Programme

Thesis Advisor: Prof. Dr. Alim Rüstem ASLAN

JUNE 2025

ISTANBUL TEKNİK ÜNİVERSİTESİ ★ LİSANSÜSTÜ EĞİTİM ENSTİTÜSÜ

6U KÜP UYDULAR İÇİN ORİGAMİ YAPILI AÇILABİLİR S-BANT SARMAL ANTEN TASARIMI

YÜKSEK LİSANS TEZİ

Rümeysa ÜSTÜNCAN
(514221036)

Savunma Teknolojileri Anabilim Dalı

Savunma Teknolojileri Programı

Tez Danışmanı: Prof. Dr. Alim Rüstem ASLAN

HAZİRAN 2025

Rümeysa ÜSTÜNCAN, a M.Sc. student of ITU Graduate School student ID 516221036, successfully defended the thesis entitled "DESIGN OF AN ORIGAMI STRUCTURED DEPLOYABLE S-BAND HELICAL ANTENNA FOR 6U CUBESATS", which he/she prepared after fulfilling the requirements specified in the associated legislations, before the jury whose signatures are below.

Thesis Advisor : **Prof. Dr. Alim Rüstem ASLAN** ....
Istanbul Technical University

Jury Members : **Asst. Prof. Dr. Hasan Bülent YAĞCI** ....
Istanbul Technical University

Asst. Prof. Dr. Erdem Onur ÖZYURT ....
Turkish-German University

Date of Submission : 27 May 2025
Date of Defense : 13 June 2025

To my family and friends,

FOREWORD

I would like to express my sincere gratitude to my advisor, Prof. Dr. Alim Rüstem ASLAN, for his irreplaceable support throughout this journey. His guidance opened a path far beyond what I could see for myself, and his influence has deeply impacted not only this project but also my life, bringing me closer to my dreams.

Special thanks to the brilliant and talented electronic engineer Ali KOCA for helping me in every step of the design and execution process.

I am deeply thankful to Asst. Prof. Dr. Hasan Bülent YAĞCI and extend my heartfelt appreciation for his belief in the potential of this project, his continuous support and willingness to dedicate time for testing the project in the anechoic chamber and as well as creating the opportunity of testing. I would also like to thank the Medical Devices Research, Development and Application Laboratory in the Faculty of Electronics for their support during anechoic chamber testing.

I am grateful to all my colleagues in the Space Systems Design and Testing Laboratory for their valuable contributions to this project Onur ÖZTEKİN, Bilge MEMİŞ, Aybüke AĞIRBAŞ, Barış BEYNEK, Kaan GÖKTÜRK, Can Görkem AKILLI, Kaan SARICA and Mehreen AZAM.

I would also like to express my appreciation to my fellow graduate students, Elif Nur YAŞAR and Şenay YENER, with whom I shared this journey. I couldn't imagine going through this process without them.

Finally, for their encouragement and continuous support, I would like to thank my dear family and close friends especially Zehra Nur AKÇALI, Nurdan Betül ÖZDEMİR ABAY, Oğuz Ulaş YAMAN and Ayşegül Selin AKSOY.

May 2025

Rümeysa ÜSTÜNCAN
(Industrial Designer)

TABLE OF CONTENT

Page

FOREWORD ... **ix**
TABLE OF CONTENT ... **xi**
ABBREVIATIONS ... **xiii**
SYMBOLS ... **xv**
LIST OF TABLES ... **xvii**
LIST OF FIGURES ... **xix**
SUMMARY ... **xxi**
ÖZET ... **xxiii**
1. INTRODUCTION ... **1**
1.1 Purpose of the Thesis ... 1
1.2 Axial and Normal Antenna ... 3
1.3 CubeSats ... 4
1.4 CubeSat Research at İTÜ ... 5
1.5 Antenna Theory ... 6
1.5.1 Introduction to antennas ... 6
1.5.1.1 How does an antenna work? ... 6
1.5.2 Fundamental parameters of antennas ... 7
1.5.2.1 Radiation pattern ... 7
1.5.2.2 Gain and directivity ... 7
1.5.2.3 Polarization ... 7
1.5.2.4 Bandwidth ... 8
1.5.2.5 Antenna efficiency ... 8
1.5.2.6 Impedance matching and the Smith Chart ... 9
1.5.2.7 VSWR ... 10
1.5.2.8 S11 parameter ... 11
1.5.2.9 Helical antenna calculation formulas ... 12
2. BACKGROUND ... **15**
2.1 RAFS Mission ... 15
2.2 RAFS Communication Plan ... 16
2.3 Satellite Communication ... 16
2.3.1 Ground station ... 16
2.3.2 Role of modems in s-band communication ... 17
2.3.3 Link budget considerations ... 18
2.3.4 Placement of the antenna on the CubeSat constrains, opportunities ... 18
2.4 Antenna Selection ... 20
2.5 Literature Review ... 24
2.5.1 Other Satellites and Their Antennas ... 25
2.5.1.1 GOMX-1 and GOMX-3 missions ... 25
2.5.1.2 Lacuna space IoT missions ... 26
2.5.1.3 CubeRRT mission ... 27

2.5.1.4 HCT QHA 28
2.5.1.5 Cat-4 mission........ 29
2.5.1.6 Skynet mission 30
2.6 Deployment Mechanism........ 33
2.6.1 Advanced deployable structural systems for small satellites........ 35
2.6.2 Truss booms 36
2.6.3 Rollable and collapsible booms........ 38
2.6.4 Origami........ 39
2.6.4.1 Kinematics of origami........ 41
3. ANTENNA DESIGN........ 43
3.1 Characteristics of the Antenna Wire........ 43
3.2 Wire Design........ 45
3.3 Comparison of Number of Turns 46
3.4 Comparison of Spacing between Turns........ 46
3.5 Feeding Mechanism........ 49
3.6 Feed structure and impedance matching 49
3.7 Material Selection........ 51
4. FABRICATION 57
4.1 The Goal of the Structure 60
4.1.1 Actuators for deployable antennas........ 61
4.1.2 Locking releasing security mechanism 61
4.2 Structure Design and Placement Requirements 64
5. SIMULATIONS AND TESTS 67
5.1 S11 Measurements........ 67
5.2 Anechoic Chamber Tests........ 70
6. CONCLUSION AND FUTURE WORK........ 75
REFERENCES........ 77
CURRICULUM VITAE 81

ABBREVIATIONS

ABS	: Acrylonitrile Butadiene Styrene
ADCS	: Attitude Determination and Control System
APSK	: Amplitude Phase Shift Keying
BER	: Bit Error Rate
EIRP	: Equivalent Isotropic Radiated Power
EQM	: Engineering Qualification Model
EPS	: Electrical Power System
FDM	: Fused Deposition Modeling
GNSS	: Global Navigation Satellite Systems
IoT	: Internet of Things
LEO	: Low Earth Orbit
LHCP	: Left-Handed Circular Polarization
Mbps	: Megabits per second
OBC	: On Board Computer
QPSK	: Quadrature Phase Shift Keying
RAFS	: Rubidium Atomic Frequency Standard
RF	: Radio Frequency
RHCP	: Right-Handed Circular Polarization
RX	: Receiver
SMA	: Shape Memory Alloy
SNR	: Signal-to-Noise Ratio
SSDTL	: Space Systems Design and Test Laboratory
TUA	: Turkish Space Agency
TX	: Transmitter
UHF	: Ultra High Frequency
UME	: Shape Memory Alloy

SYMBOLS

λ (lambda)	: Wavelength
D	: Diameter of the helix
S	: Spacing between helix turns
N	: Number of turns in the helical antenna
dBi	: Decibels over isotropic radiator
θ (theta)	: Rotation angle around the z-axis (origami kinematics)
Fa	: Axial force (strain energy/elasticity section)
***ƒ* or f**	: Frequency
Zin, Zout	: Input and output impedance
η (eta)	: Antenna efficiency
Δf	: Bandwidth or frequency range
α, β	: Phase or propagation constants
h	: Height
R	: Radius
T	: Tension or force
Z	: Impedance
Ω(Ohm)	: Unit of electrical resistance or impedance

LIST OF TABLES

Page

Table 1.1 : Antenna design considerations [12]. **2**
Table 1.2 : Comparison of normal-mode vs. axial-mode helical antennas. **3**
Table 1.3 : Size and mass of CubeSats. **5**
Table 2.1 : IEEE standard letter designations according to their frequency bands [4]. **19**
Table 2.2 : Comparison of comprehensive antenna types and characteristics. **23**
Table 2.3 : Performance of conical spiral and helical antennas [4]. **24**
Table 2.4 : Simulated gain comparison according to number of turns of the bifilar skeleton SHA. **25**
Table 3.1 : Design parameters. **45**
Table 3.2 : Comparison of number of turns. **46**
Table 3.3 : Comparison of spacing between turns. **46**
Table 3.4 : Center frequency tuning. **47**
Table 3.5 : Comparison of width of strip. **50**
Table 3.6 : Material properties comparison. **53**
Table 3.7 : Comparison table for different origami antennas [31]. **54**

LIST OF FIGURES

Page

Figure 1.1 : Different CubeSat standards. 4
Figure 1.2 : Popularity of CubeSat mission types from 2003 to 2022[4]. 5
Figure 1.3 : ITUpSAT-1, First CubeSat launched from SSDTL and Türkiye. 6
Figure 1.4 : Antenna basics. 7
Figure 1.5 : Wave polarization [11]. 8
Figure 1.6 : The standard Smith Chart. 9
Figure 1.7 : Impedance matching demonstrated by a Smith Chart. 9
Figure 1.8 : VSWR setup spectrum analyzer. 11
Figure 1.9 : A sample S11 graph. 11
Figure 1.10 : Helical antenna with ground plane [12]. 12
Figure 2.1 : RAFS configuration. 15
Figure 2.2 : RAFS concept diagram. 16
Figure 2.3 : S-band reflector antenna (UHUZAM). 17
Figure 2.4 : Altitude-classification geocentric orbits. 19
Figure 2.5 : Antenna types according to gain level. 20
Figure 2.6 : Common antenna types (a) monopole/ dipole antenna (b) patch antenna (c) meshed patch antenna (d) helical antenna. 21
Figure 2.7 : Antenna selection according to missions [4]. 22
Figure 2.8 : Relationship between number of turns and gain – HPBW. 25
Figure 2.9 : GOMX-1 with deployed antennas. 26
Figure 2.10 : ADS-B mission concept design. 26
Figure 2.11 : Lacuna space configuration. 27
Figure 2.12 : CubeRRT. 28
Figure 2.13 : HCT QHA deployment mechanism components. 29
Figure 2.14 : HCT QHA hold down and release mechanism. 29
Figure 2.15 : Hold-down folder fingers. 30
Figure 2.16 : Deployed configuration of 1U Cubesat Cat-4. 30
Figure 2.17 : Skynet configuration. 31
Figure 2.18 : Deployable helical antenna a) fully stowed b) fully deployed. 31
Figure 2.19 : The manufactured prototype of origami SHA at (a) LHCP and (b) 32
Figure 2.20 : (a) Expanded telescoping central axis, (b) collapsed telescoping central axis (c) tightly folded origami SHA. 32
Figure 2.21 : Fabricated mockup of the (a) hexagon structure SHA, (b) square skeleton SHA, and (c) conventional HA. 33
Figure 2.22 : Bifilar foil structured origami helical antenna. 33
Figure 2.23 : International Space Station (ISS). 36
Figure 2.24 : Rod-controlled deployment steps. 37
Figure 2.25 : Truss boom deployment principle. 37
Figure 2.26 : Telescopic mechanism. 37
Figure 2.27 : Antenna and satellite configuration [43]. 38
Figure 2.28 : Boom geometries. 38

Figure 2.29 : Rollable boom mechanism. **38**
Figure 2.30 : GOSSAMER-1 solar sail developed by DLR. **39**
Figure 2.31 : Kresling drawing. **40**
Figure 2.32 : The James Webb telescope. **41**
Figure 2.33 : Schematics of axial motion with rotation angle. **42**
Figure 3.1 : S11 return loss plot. **44**
Figure 3.2 : HFSS model of helical antenna. **44**
Figure 3.3 : HFSS simulation results in s-band. **45**
Figure 3.4 : Simulated gain plot of the antenna design. **48**
Figure 3.5 : Simulated beamwidth of the antenna. **48**
Figure 3.6 : Simulated radiation pattern of the antenna design. **48**
Figure 3.7 : Impedance matching strip. **50**
Figure 3.8 : Manufactured strip soldered to SMA connector and conductor antenna wire. **50**
Figure 3.9 : Conductive materials for fabricating origami antennas. **51**
Figure 3.10 : Dielectric materials for fabricating origami antennas [44]. **52**
Figure 3.11 : SMA connector with ground plane. **55**
Figure 4.1 : Mockups during process. **57**
Figure 4.2 : Stowed version of antenna (45 mm). **58**
Figure 4.3 : Deployed version of antenna (176 mm). **59**
Figure 4.4 : 2D drawing of the polyamide sheet. **59**
Figure 4.5 : Exploded CAD model of antenna. **60**
Figure 4.6 : Employed dyneema wire. **61**
Figure 4.7 : 3D printed structure parts. **62**
Figure 4.8 : Cross-section of the stowed elbowed boom. **62**
Figure 4.9 : Hold and release mechanism of the helical antenna. **63**
Figure 4.10 : Relationship between the antenna structure and dyneema wire. 63
Figure 4.11 : Storage Stability Test Model. **63**
Figure 4.12 : 6U CubeSat Dimension [41]. **64**
Figure 4.13 : Rendering of deplored version of helical origami antenna with 6U CubeSat configuration. **65**
Figure 5.1 : S11 spectrum results. **67**
Figure 5.2 : The test setup antenna. **68**
Figure 5.3 : Initial S11 spectrum testing of the antenna. **69**
Figure 5.4 : Spectrum testing with origami structured helical antenna. **70**
Figure 5.5 : Anechoic chamber test environment. **71**
Figure 5.6 : Pyramidal RAM absorbs the incident signal. **71**
Figure 5.7 : Calibration of the spectrum analyzer. **72**
Figure 5.8 : The test setup with origami structured helical antenna. **73**
Figure 5.9 : Network analyzer test results. **73**

DESIGN OF AN ORIGAMI STRUCTURED DEPLOYABLE S-BAND HELICAL ANTENNA FOR 6U CUBESAT

SUMMARY

This study covers the design, simulations, tests, and prototyping process of a deployable S-band helical antenna for 6U CubeSats. The antenna was developed to provide high gain and circular polarization. Furthermore, compactly stored and reliably deployed within the satellite and designated to operate in the 2- 4 GHz frequency range with 2267 MHz center frequency. The antenna has a target gain of 10 dB which is a promising RF characteristic to achieve efficient satellite communication.

Factors such as assembly, deployment mechanism, cost, weight, placement on the CubeSat configuration are examined and explained through the design decisions. Silver-plated aluminum, gold-plated titanium and copper were considered as conductive materials in the design, while polyamide film is preferred as mechanical structure materials during material selection process. The deployment mechanism was designed to be reliably deployed with the contribution of potential energy stored in the helical wire and origami structure. The relationship between the wire antenna and is Kapton® 300 HN polyimide film as a foldable origami-based structure, which increases its compactness and deployability is developed.

To verify the RF performance of the wire design, electromagnetic simulations were performed and analyzed in ANSYS HFSS software such parameters as radiation pattern, impedance matching and return loss (S11). The feasibility of the deployment mechanism was provided and evaluated with mechanical and kinematic modeling conducted in CATIA software. Then, 3D printed prototypes were produced and tested with spectrum analyzer and, after that, in an anechoic chamber. Tests were applied to examine the antenna operability and solidity in space environment.

The results of the study are obtained that the helical antenna provides high gain and circular polarization and it is a suitable candidate for CubeSat communication systems for deep space and Earth observation missions. In addition to developing a good balance between size, gain and directivity, it is emphasized that a reliable deployment mechanism is a critical design component.

As future work, alternative structures such as quadrifilar helix (QHA) or log-periodic antennas are also planned to be considered and compared in terms of performance optimization, producing the antenna as a space-qualified product to be launched into space after conducting necessary environmental testing such as TVAC (thermal vacuum chamber) and considering the different kinds of conductive materials to conduct better RF performance.

6U KÜP UYDULAR İÇİN ORİGAMİ YAPILI AÇILABİLİR S-BANT SARMAL ANTEN TASARIMI

ÖZET

Küp uydular; üniversiteler, şirketler ve öğrenci grupları için uzaya erişimi ve uzayın sağlayabileceği imkanlardan faydalanmayı mümkün hale getiren nano uydu sistemleridir. Bu uydular, yeryüzü gözlemi, telemetri ve veri aktarımı ile data erişimi gibi çeşitli görevlerle görevlendirilir. Bu yeteneklerin mümkün olabilmesi, yer istasyonu ile uydu arasında güvenilir bir iletişim sağlanmasına bağlıdır. Verimli bir iletişimi mümkün kılan temel unsurlar ise elektromanyetik dalgaları elektrik sinyallerine dönüştüren antenlerdir.

Bir küp uydunun sahip olduğu görev tanımı, anten sisteminden beklenen performans kriterlerini doğrudan belirler. Örneğin, yönsüz (omnidirectional) antenler geniş kapsama alanı sunarak düşük yönlü kazançla her yöne sinyal yayılımı sağlarken; yönlü (directional) antenler, enerjiyi belirli bir doğrultuda yoğunlaştırarak daha uzun menzilli ve yüksek hızlı ve kaliteli iletişim kurma avantajı sağlar. Bu sebeple, antenin türü ve yapısal özellikleri, anten tasarım sürecinin en önemli karar noktalarından biridir. Her anten türünün kendine özgü avantaj ve sınırlamaları bulunmakta olup, görev ihtiyaçlarına en uygun çözümün seçilmesi sistem performansı açısından belirleyicidir.

Yüksek kazançlı antenler, sinyal gücünü artırarak iletişim kalitesini ve veri aktarım hızını optimize eder. Dolayısıyla sarmal(helical) antenler, dairesel polarizasyon yetenekleri, geniş bant genişliği ve yüksek kazanç gibi küp uydu haberleşmesi için gerekli nitelikleri bir arada sunmaları açısından öne çıkmaktadır. Helisel antenler, kavisli formları ve helisel yapıları nedeniyle doğal olarak dairesel polarizasyon sergileme avantajına sahiptir. Bu proje, antenin dalga boyu, çapı ve antenin zemin düzlemi gibi yapısal ve elektriksel özelliklerinin çoğunu tanımlayan belirlenmiş frekansı hedeflemektedir. Bu özellikler, helisel antenlerin yönlülük sağlaması ve uyduyu yer istasyonuna hedeflemesi için bir zorunluluktur. Kazanç, yönlülük ve mesafe sınırlamaları gibi iletişim gereksinimleri de belirlenen diğer özelliklerdir. Küp Uydular sınırlı alana sahip olduğundan, anten boyutu, kazanç ve yönlülüğün dengelenmesi özellikle zorlu ve gerekli bir yaklaşımdır.

Sarmal antenler spiral şeklindeki yapıları sayesinde açılabilir özellikte olabilirler. Açılabilir antenlerin tasarımı karmaşıktır ve davranışları uzay koşulları altında kesin olarak tahmin ve kontrol edilemez, ancak başarılı uygulamalar iletişim kabiliyetini ve genel CubeSat performansını önemli ölçüde artırır. Antenler başlangıçta uzay aracının içine katlanmış halde yerleştirilir ve uzaya çıktıktan sonra açılır, bu nedenle güvenilir bir açılma mekanizması kritik öneme sahiptir.

Bu çalışmada, 6U küp uydular için açılabilir S-bant sarmal anten tasarımı, simülasyonları ve testleri ele almaktadır. Anten, yüksek kazanç ve dairesel polarizasyon sağlarken, uydu içerisinde kompakt bir şekilde saklanabilmesi ve güvenilir bir şekilde açılabilmesi amacıyla geliştirilmiştir. 2-4 GHz frekans aralığında

çalışmak üzere tasarlanan antenin merkez frekansı 2267 MHz olup, hedef kazancı 10 dB'dir; bu da verimli uydu haberleşmesi için umut vaad eden bir RF özelliğidir.

Tasarımın RF performansı antenin araç performansı antena teorisi formüllerinden yola çıkılarak hesaplanmıştır. Dalga boyu frekansa bağlıdır dolayısıyla frekansa bağlı olarak antenin çapı kazanç ve yönlülük miktarına göre simülasyonlarla belirlenmiş ve optimize edilmiştir. Bu doğrulamak için de ANSYS HFSS yazılımında elektromanyetik simülasyonlar gerçekleştirilmiş. Işınım deseni, VSWR (Gerilim Dalgası Durum Oranı), kazanç, empedans eşleşmesi ve yansıma kaybı (S11) gibi parametreler analiz edilmiştir.

Anten seçimi, yama, sarmal, konik, log-periyodik, quadrifilar sarmal (QHA) ve diğer açılabilir yapıların karşılaştırılması yoluyla yapılmıştır. Yama antenler daha basit ve maliyet açısından avantajlıdır, bu nedenle pek çok uygulamada tercih edilir. Ancak sarmal antenler, doğal dairesel polarizasyon, daha yüksek kazanç ve geniş bant genişliği gibi üstün özellikler sunar, bu da onları yüksek performanslı iletişim görevleri için daha uygun kılar. İyi tasarlanmış ve optimize edilmiş bir açılma mekanizması ile helisel antenler üstün performans sağlayabilir. Temel anten denklemleriyle yapılan teorik hesaplamalar, ilk sonuçları belirlemeye ve boyutları optimize etmeye yardımcı olur.

Origami yapının kinematik özellikleri Castigliano teoremiyle açıklanmış, deformasyon sonucu oluşan gerilme enerjisi hesaplanmıştır Minimum potansiyel enerjili kesişme noktaları kuvvetin sıfır olduğu denge konumları haline gelmiş ve harici bir güce ihtiyaç duyulmadan açılır bir yapı oluşturulmuştur. Yapının kendisi bir yay özelliği taşımıştır. Açılma mekanizması doğal katlama teknikleriyle tasarlanmıştır. Açılabilirliği sağlayan mekanik yapı malzemesi olarak ise poliamid film tercih edilmiştir. Açılma mekanizması, sarmal telde ve origami yapısında biriken potansiyel enerjinin katkısıyla güvenilir bir şekilde açılacak şekilde tasarlanmıştır. Buna ek olarak katlanabilir bir origami yapısı oluşturan Kapton® 300 HN poliamid film ile kaplanarak kompaktlık ve açılabilirlik özellikleri artırılmıştır. Ayrıca bu açılma mekanizması için kilitleme ve serbest bırakma mekanizması direnç ve yanıcı tel yöntemiyle gerçekleştirilmiştir. Bu kilitleme ve serbest bırakma sistemi, yüksek güvenilirlik sunmaktadır ve uzay görevleri için uygun bir çözüm olarak değerlendirilmiştir.

Açılma mekanizmasının uygulanabilitliği ise CATIA yazılımında yapılan mekanik ve kinematik modellemelerle değerlendirilmiştir. Ardından, 3B yazıcı ile prototipler üretilmiş. Spektrum analizörü ile ve sonrasında yankısız odada test edilmiştir. Bu testler, antenin uzay ortamında çalışabilirliğini değerlendirmek amacıyla gerçekleştirilmiştir.

Maliyet, ağırlık ve küp uydu konfigürasyonu üzerindeki yerleşimi gibi faktörler tasarım kararları aracılığıyla ayrıntılı şekilde incelenmiş ve açıklanmıştır. Tasarım sürecinde iletken malzeme olarak gümüş kaplamalı alüminyum, altın kaplamalı titanyum ve bakır değerlendirilmiştir. Her bir malzeme radio frekansı performansı, iletkenlik, korozyon direnci, uzay ortamı ile uyumluluk ve üretilebilirlik açısından karşılaştırılmıştır. Zemin düzleminin amacı antenin yünlülük özelliği kazandırmak olduğu için alüminyum tercih edilmiştir.İletken anten sarmalı için gümüş kaplamalı bakır malezeme kullanılmıtır Bu malzeme ek olarak yapıya destek olabilecek direngenlik özelliği de göstermektedir.Impedans eşleme parçası için yine iyi bir iletken olan bakır kullanılmıştır ve güç kaynağıyla bağlantı noktası olarak SMA konnektör kullanılmıştır.

Çalışmanın sonuçları, tasarlanan sarmal antenin yüksek kazanç ve dairesel polarizasyon sağladığını; hafif, kompakt, verimli ve yönlü özellikleri taşıdığı ve küp uydu haberleşme sistemleri ile derin uzay ve yer gözlem görevleri için uygun bir aday olduğunu göstermektedir. Boyut, kazanç ve yönlülük arasında iyi bir denge sağlanmasının yanı sıra, güvenilir açılma mekanizmasının kritik bir tasarım faktörü olduğu vurgulanmaktadır.

Aynı zamanda sarmal antenin uydu üzerindeki yerleşimi de küp uydu standartlarına uygunluğu göz önünde bulundurulmuş, antenin katlanmış hâli 40 × 35 mm boyutlarında olacak şekilde tasarlanmıştır; bu da uydu dışında kalınabilecek 80 × 40 mm aralığında kalması gereken sınırlar içinde yer almaktadır. Bu ölçülerin fırlatma kapsülüne (POD) sığması, yapısal tasarım açısından önemli bir kriterdir.

Gelecekte, dört iletkenli (quadrifilar) sarmal (QHA) antenler veya log-periyodik antenler gibi alternatif yapıların farklı malzemelerle de performans optimizasyonu açısından incelenmesi ve antenin TVAC (termal vakum odası) ile vakum döngüsü, gaz salınımı (outgassing) ve fonksiyonel testler gibi çevresel testlerden geçirilerek uzay yeterlilik seviyesine uygun bir endüstriyel ürün haline getirilmesi ve antenin ve açılma mekanizmasının uzay performansının da değerlendirilmesi planlanmıştır.

1. INTRODUCTION

1.1 Purpose of the Thesis

The purpose of this thesis is to conduct and suggest an antenna design to provide the signal power, directivity and accuracy for 6u CubeSat design, followed by a detailed discussion of its design, simulating, prototyping and testing.

First chapter summaries antenna theory and existing solutions. Second design specifications are explained limitations and solutions. Material and antenna selection form and mechanism selection detailly discussed in belonging chapter. In the final chapter, results of tests and simulations conclusion, solutions, inferences potential and future work are ventilated. Deployable space structures are challenging and complicated to design and test environments that deliver results in high confidence that convincing about the component will deploy correctly in space.

Deployable antenna configurations must be considered in case the necessity of larger antenna volume is required for mission. If an anomaly occurs in space, there are limited options to correct the condition. This thesis will investigate current research and development into deployable CubeSat antennas and will devise and evaluate the steps required to verify and characterize the space performance of a proposed deployable helical antenna for RAFS CubeSat mission by considering the characteristics in Table 1.1.

Table 1.1 : Antenna design considerations [12].

Current Challenges	Performance
High gain	• Intersatellite communications • Deep space missions • High speed data downlink
Wide bandwidth and Multiband	• Increased throughput • Single antenna operating at different frequencies (i.e., up/downlink) • Remote Sensing applications
Small size and low mass	• Low cost, fast prototyping • Sufficient real estate for solar panels • Reduce weight budget
Circular polarization	• Eliminating polarization mismatch losses due to antenna misalignment • Reduce the effect of Faraday rotation • High link reliability • Intersatellite communication

The goal of this thesis is to qualify the HCT QHA design by developing and conducting testing procedures that characterize the antenna's deployment performance and verify the antenna will meet or exceed the defined operability and survivability limits. Every satellite mission depends on radio frequency (RF) communications to receive and transmit data. CubeSat missions, such as accomplishing reliable communication and supplying imagery outcome, causes plenty of data. To handle this amount of data, CubeSat must have efficient RF attributes high gain, wide bandwidth and beamwidth.

These RF attributes can be achieved through various components of the satellite communications subsystem. Antennas are potential components of the satellite communications (SATCOM) architecture that could provide additional capability, without placing demands on power and computer processing. A challenging aspect of CubeSat antenna configurations is small and preserved volume for antennas on CubeSat as available face for placing the antenna will become a larger antenna.

Deployable space structures carry the risk of uncertainty about their behavior in the space to eliminate the risk design and test process must have the maximum reliability. Because when an error occurs, it is normally not solvable or limited possibilities exist. Therefore, systems are designed according to no risk configurations like patch or parabolic antennas but the opportunities that deployable systems provide cannot be ignored. More research should be conducted into deployable systems. Achieving a high gain while having a small size is one of the keys aims while antenna design process [4].

1.2 Axial and Normal Antenna

Spacing between turns changes the mode of antenna it can be axial and normal. between 0.2–0.25λ exhibit axial radiation and circular polarization. (e.g., Kraus, 1950s). 022λ good axial ratio and good impedance match as summarized in Table 1.2.

The spacing provides the phase delay between turns produces radiation which means waves add constructively along the axis. Typically, the helical antenna diameter is obtained from the result of the division of wavelength and π [12].

Table 1.2 : Comparison of normal-mode vs. axial-mode helical antennas.

Parameter	Normal-Mode Helix	Axial-Mode Helix
Operation	Resonates when length ≈ λ/4 or λ/2 (like a monopole).	Radiates along the helix axis (end-fire).
Dimensions	- D << λ (thin helix). - S << λ (tightly spaced turns).	- D ≈ λ/π (~0.318λ). - S ≈ 0.22λ.
Polarization	Linear (parallel to helix axis).	Circular (handedness depends on winding direction).
Impedance	Low (~50 Ω), easily matched to coax.	High (~100–150 Ω), often requires matching.
Radiation Pattern	Omnidirectional (broadside).	Directional (main lobe along axis).
Gain	Low (~1–3 dB).	Moderate to high (~10–15 dBi for 10+ turns).
Applications	RFID tags. Compact antennas for portable devices.	Satellite comms. GPS, radar, high-gain links.

According to Kraus, in normal mode, a helical antenna can be defined as a monopole antenna which has a helical loading element, serving dominant radiation is linearly polarized and perpendicular to axis (Kraus & Marhefka, 2002). However, since the helix diameter reduces too drastically, efficiency diminishes. It causes the loss of monopole-like behavior.

On the other hand, non-resonant broadband behavior is achieved by the axial mode. In this mode, gain enhances in every turn which is for each turn around ~1.5–3 dB until 12 turns. As antenna options, normal mode antennas which are small and linearly polarized antennas can be used in cases where spacing is limited. Axial mode antennas should be used for the cases high gain is required and circularly polarized systems with high data rate and complex payload mission communication.

1.3 CubeSats

Satellites have scaled down thanks to the development in space technologies. 10 cm3 cube shape configurations as visualized in Figure 1.1 and Table 1.3. CubeSats are nano-class satellites, and they are used for space research. With CubeSat's low manufacturing and launch costs, there is an increased interest in using CubeSats for national defense, homeland security and disaster response [1]. These uses require a CubeSat's payload to have cameras to capture pictures and videos. Many space projects in university laboratories are focused on the development of small satellites for both scientific and educational purposes as summarized in Figure 1.2.

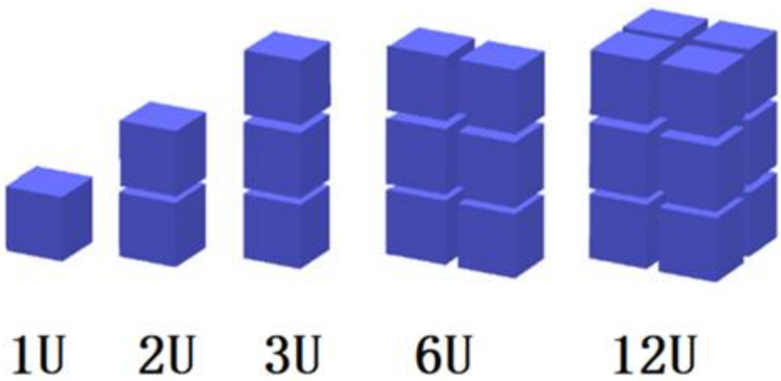

Figure 1.1 : Different CubeSat standards.

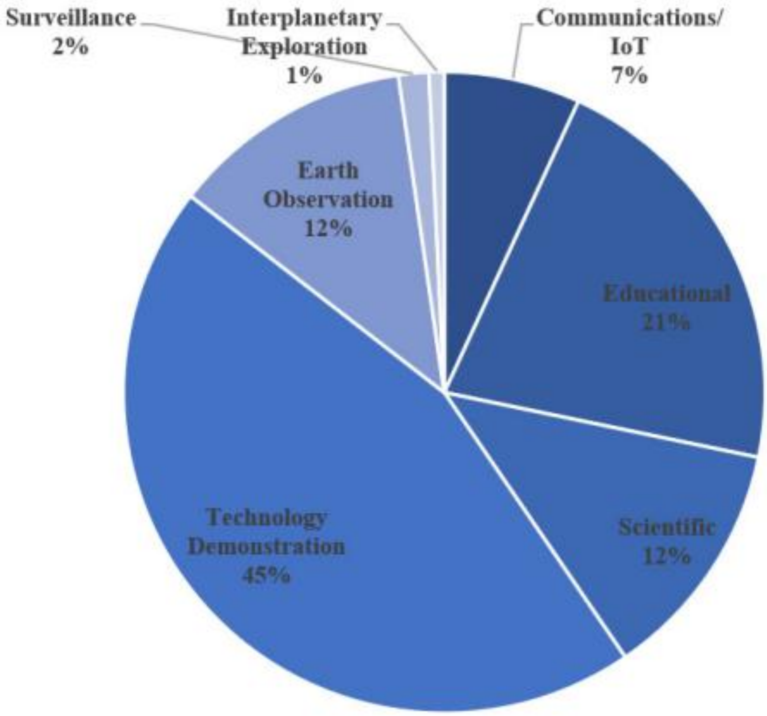

Figure 1.2 : Popularity of CubeSat mission types from 2003 to 2022[4].

Table 1.3 : Size and mass of CubeSats.

Size	Dimensions (cm)	Wet Mass (kg)
1U	10 × 10 × 10	1.3
2U	10 × 10 × 20	2.6
3U	10 × 10 × 30	3.9
6U	10 × 20 × 30	7.8
12U	10 × 10 × 60	15.6

1.4 CubeSat Research at İTÜ

This thesis is written with the contributions of Space Systems Design and Testing Laboratory (SSDTL) which is located at Istanbul Technical University (ITU) is a pioneer for CubeSat research, being one of the first in the world and the very first in Türkiye to develop a CubeSat with ITUpSAT-1 shown in Figure 1.3. Since its establishment in 2007, SSDTL has designed, tested, and launched seven other CubeSats and keeps going their journey developing remarkable systems.

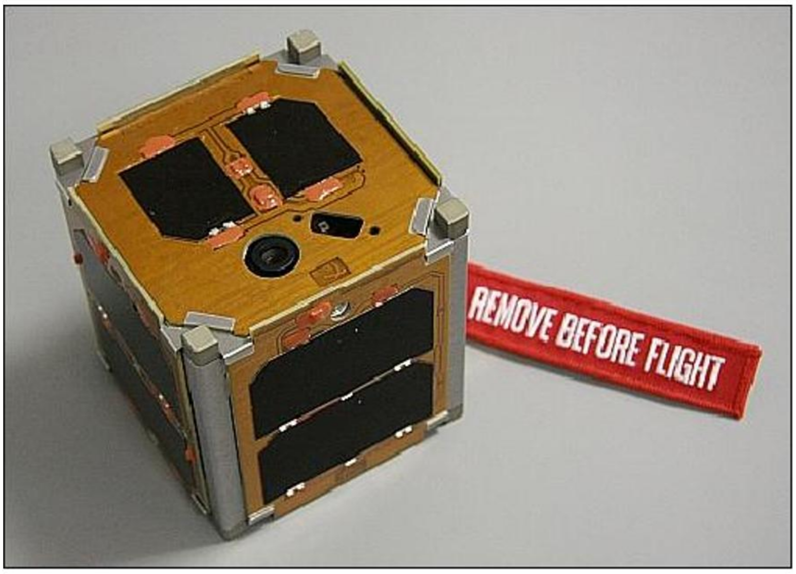

Figure 1.3 : ITUpSAT-1, First CubeSat launched from SSDTL and Türkiye.

1.5 Antenna Theory

1.5.1 Introduction to antennas

1.5.1.1 How does an antenna work?

Antennas contribute a range of abilities and functions depending on their mission, type and design. Every type has their own opportunities and challenges to overcome. The basic characteristic of antennas is to behave like an interface between electrical signals and electromagnetic waves. Especially for deployable antenna systems, implementation of antenna theory with mechanical structure is vital. Basic functions of antennas are to alter electromagnetic waves into electrical signals. Antennas with high directional behavior need constantly aligned transmitter and receiver to sustain the quality of the signal. A transmitting antenna functions as a device converts a guided electromagnetic signal wave operates by travelling along a guided pathway into a radiated plane wave that propagates through deep space or a receiving antenna [3]. Meanwhile antennas are bidirectional which means they can both transmit and receive signals which is a desirable feature. One end of the antenna behaves like an electrical circuit connection element, while the other side provides an interface with the surrounding electromagnetic environment with a propagating plane wave. A schematic in Figure 1.4 illustrates the fundamental interface basics of this principle.

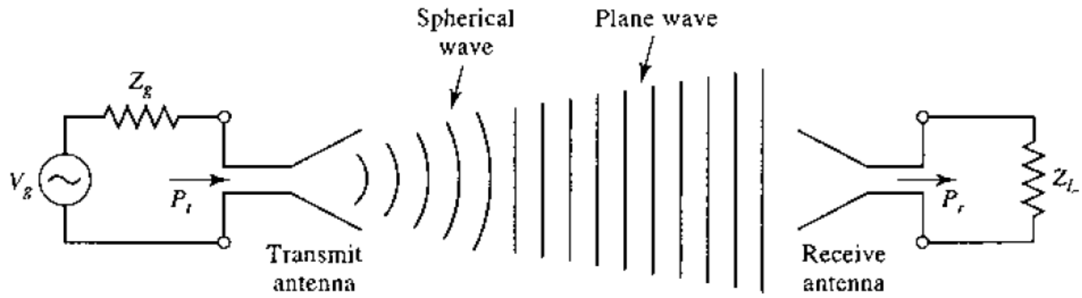

Figure 1.4 : Antenna basics.

1.5.2 Fundamental parameters of antennas

1.5.2.1 Radiation pattern

In the axial mode (technical name end-fire mode), the antenna radiates along beam axis in a high directional behavior which produces circularly polarized radiation pattern which idealizes the satellite communication since it provides the antenna to transmit and receive signals from the satellite while maintaining signal strength consistently without depending on the orientation of receiving and transmitting antennas relatively. Flux density, radiation intensity, polarization are some of the elements of radiation pattern.

1.5.2.2 Gain and directivity

Gain means the capability for directing the radiated energy into a preferred specific direction, which increases the power and clarity of signals and enhances the performance for longer distance missions. It consists of both the directivity and the efficiency which means the amount of the radiated power which is transmitted efficiently. The clarity, power and the range of power is influenced by efficiency.

Directivity is defined with the geometry of the helix specifically number of turns, diameter of helix and spacing between turns. In axial mode, the antenna radiates in a narrow beam along its axis which makes the antenna highly directive and affects the gain drastically positively.

1.5.2.3 Polarization

There are two types of polarization which are linear and circular polarization as demonstrated in Figure 1.5 in the coordinate system. The reason is that the ionosphere causes Faraday rotation to an electromagnetic wave, depending on thickness and temperature of the ionosphere the rotation is high at lower frequencies makes linear polarization very hard to match after passing ionosphere, but circular polarization doesn't jeopardize the communication on the contrary supports it. Polarization also can be defined as right hand and left-hand polarization. There are various crucial advantages of using circular polarization for space systems while they are simplified antenna alignment reflection and multi band resistance frequency band sharing installation it is not necessary to align antenna rotationally because it says circularly polarized antennas naturally rotate to the aligned. Right and left hand can be used to transmit two separate signals in the same frequency band, but the polarization should be matched transmitted signals and the receive themed and vice versa for reflection and multipath resistance [11].

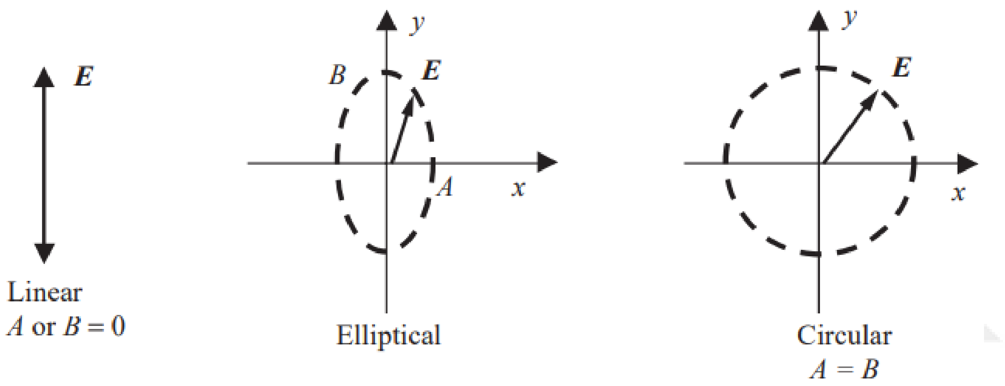

Figure 1.5 : Wave polarization [11].

1.5.2.4 Bandwidth

Bandwidth can be summarized as the range of frequencies the antenna functions. It defines the amount of difference from the center frequency is acceptable for the operation.

1.5.2.5 Antenna efficiency

The total efficiency of the antenna is related to reflection efficiency, conduction efficiency, dielectric efficiency, voltage reflection coefficient at the input terminals of the antenna input impedance and characteristic impedance of the transmission line [13].

1.5.2.6 Impedance matching and the Smith Chart

$$\text{VSWR} = \text{voltage standing wave ratio} = \frac{1+|\Gamma|}{1-|\Gamma|} \qquad (1.1)$$

The VSWR value is obtained with absolute value of Γ voltage reflection coefficient at the input terminals of the antenna.

It can be defined as the antenna resistance to the terminals, the ratio of the voltage to current at a pair of terminals or the ratio of the appropriate components. It defers according to geometry, the environment around, excitation.

In figures 1.6 and 1.7 below, The Smith Chart, which is studied by Philip H. Smith and it has the ability for visualization of so many parameters such as complicated impedance reflection coefficients behaviors through RF circuits, it is used for stability analysis and oscillator design.

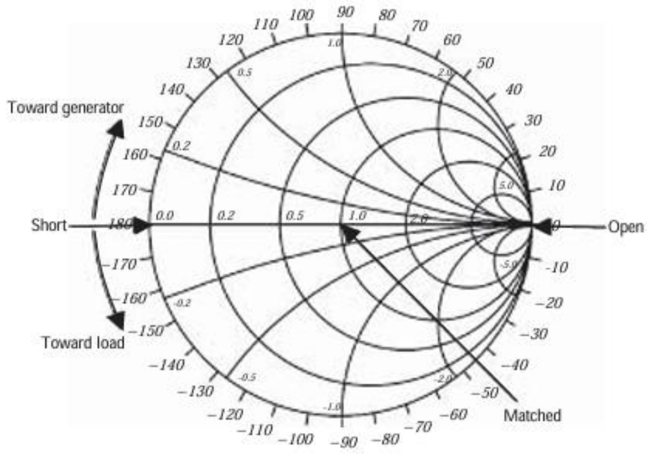

Figure 1.6 : The standard Smith Chart.

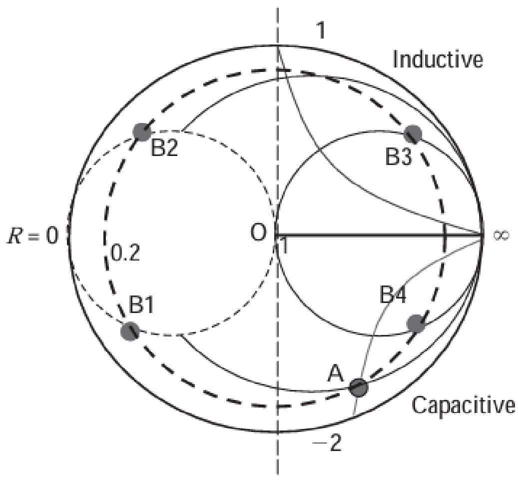

Figure 1.7 : Impedance matching demonstrated by a Smith Chart.

Impedance matching refers to equalizing practice of the output and input impedance to maximize the power transferring provided by the antenna and diminishing the reflections from the load as much as possible [12].

To ensure maximum power transfer between the antenna and the transmission line, impedance matching is required. This is achieved when the source impedance Z_S is equal to the complex conjugation of the load impedance Z_L . Mathematically, this condition is expressed as:

$$Z_S = Z_L^* = \left(R_L + JX_L\right)^* = R_L - JX_L \tag{1.2}$$

Here, Z_S is the source impedance, Z_L is the load impedance, R_L is the resistive component of the load, and X_L is the reactive component and where J is the imaginary unit. The asterisk (*) denotes the complex conjugate. This matching ensures that reactive components cancel out, and the maximum amount of power is transferred from the source to the antenna.

1.5.2.7 VSWR

VSWR expresses the ratio of the maximum voltage amplitude of a standing wave along the transmission line to the minimum amplitude of a standing wave from input voltage. In fully efficient scenario for VSWR measuring should be 1.0, which means there is no radiated energy turning back as a reflection into the RF transmission pathway from the antenna. VSWR testing provides an outcome for the influence of design of the antenna geometry to the power and RF performance of the antenna at a certain frequency by examining impedance matching between the source and load. If the radiated power deviates substantially, it may lead to changes in the antenna's RF performance characteristics. Beam pattern or gain value should be known to perform this test. The VSWR test setup is demonstrated in Figure 1.8. The center frequency is set to 2267 MHz and with bandwidth is set to 50 MHz.

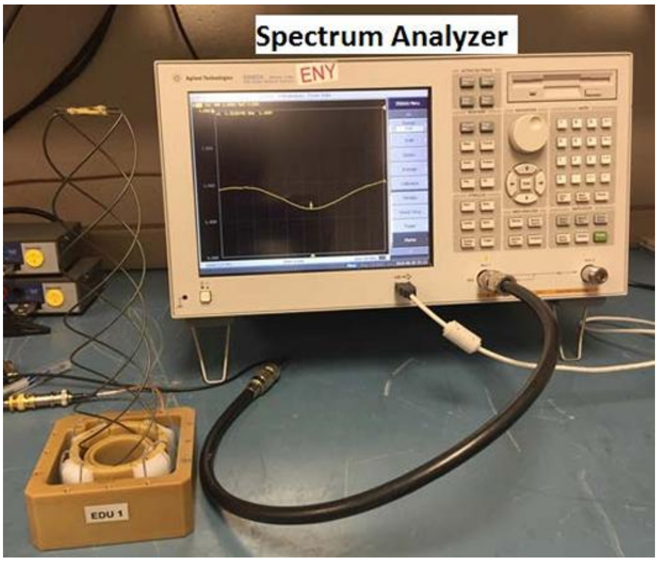

Figure 1.8 : VSWR setup spectrum analyzer.

1.5.2.8 S11 parameter

The S11 parameter can be seen in Figure 1.9 represents the reflection coefficient, measuring the power reflecting to the source from the antenna back due to the impedance mismatch. It is a parameter about whether the power entrances and delivers to antenna efficiently. The more negative the value, the more powerful the antenna performance is in terms of signal reception or transmission. Under the value – 10 dB means the antenna works and the dips show which frequency it works at the best condition. It clearly demonstrates the impedance matching level of the antenna, assists to analysis of bandwidth and resonance characteristics and evaluation of the antenna gain, reflection and isolation performance.

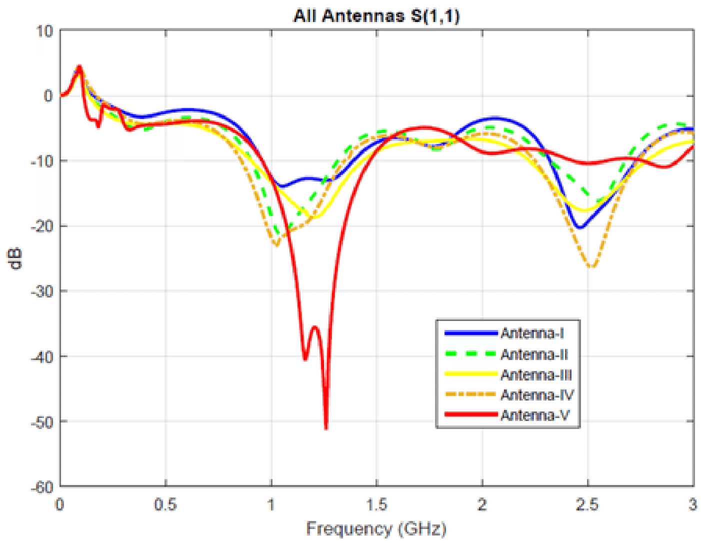

Figure 1.9 : A sample S11 graph.

1.5.2.9 Helical antenna calculation formulas

A helical antenna demonstrated in Figure 1.10 is characterized by several key geometric and performance parameters. The number of turns, denoted as N, defines how many complete revolutions the wire makes around the helix. D represents the diameter of the helix, while the spacing S is the axial spacing between each turn, λ is the wavelength and f sembolizes frequency [15].

Another important parameter is the pitch angle α which is the angle formed by a line tangent to the helix wire and a plane perpendicular to the helix axis.

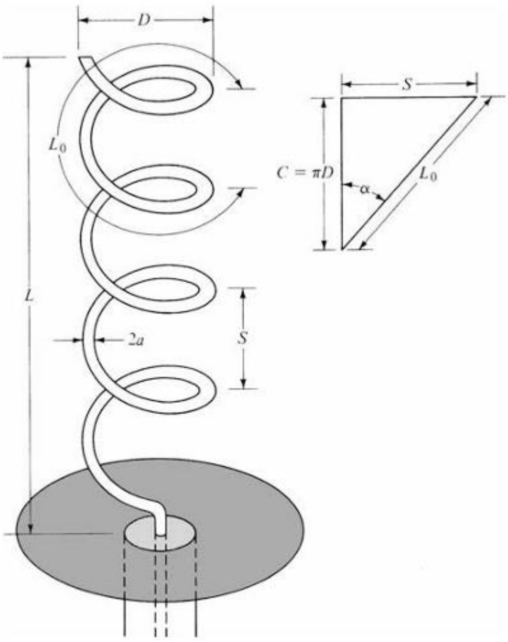

Figure 1.10 : Helical antenna with ground plane [12].

Impedance,

$$R \simeq 140\left(\frac{C}{\lambda^0}\right)\ relevant\ for \pm 20 \quad (1.3)$$

The half power beamwidth,

$$HPBW(degrees) \simeq \frac{52\lambda_0^{3/2}}{C\sqrt{NS}} \quad (1.4)$$

The beamwidth between by nulls,

$$HPBW(degrees) \simeq \frac{115\lambda}{C\sqrt{NS}} \quad (1.5)$$

Directivity,

$$D_0 \simeq 15N\frac{C^2S}{\lambda_0^3} \quad (1.6)$$

The axial ratio,

$$AR = \frac{2N+1}{2N} \tag{1.7}$$

The total axial length of the antenna is the multiplication,

$$L = NS \tag{1.8}$$

while the total length of the wire is,

$$L_{n} = NL_0 = N\sqrt{S^2} + C^2 \tag{1.9}$$

Where,

$$L_0 = \sqrt{S^2} + C^2 \tag{1.10}$$

is the length of the wire between each turn and.

$$C = \pi D \tag{1.11}$$

is the circumference of the helix.

The pitch angle is defined by,

$$\alpha = tan^{-1} S\, \pi \tag{1.12}$$

$$D = tan^{-1} S\, C \tag{1.13}$$

Bandwidth,

$$f_{low} = f_{center} - \frac{bandwidth}{2} \tag{1.14}$$

$$f_{high} = f_{center} + \frac{bandwidth}{2} \tag{1.15}$$

2. BACKGROUND

2.1 RAFS Mission

A 6U structured CubeSat with a main payload Rubidium Atomic Frequency Standard (RAFS) visualized in Figure 2.1. This configuration is in the course of development by the collaborative work TUBİTAK UME, ITU SSDTL (Space Systems Design and Test Lab.) and ITU RF Lab., for Turkish Space Agency (TUA). Main mission is to accommodate the main payload which is RAFS with the mission of GNSS timing, producing and testing by TUBITAK UME. Some secondary payloads measurement cards and camera in space and keep it safe which is a is a national project supported by domestic institutions. Main purpose is to provide accurate time as native for GNSS systems. The system mainly consists of EPS, OBC as computer, ADCS as attitude determination and control component and camera. It is planned to test payload in LEO (Low Elevation Orbit) orbit with 6U CubeSat structure.

After launch, the actions of RAFS assembled onto the such as aging, stability features will be analyzed in the space environment. Therefore, to accomplish this, the time base of communication frequency is designated in the range of 10 MHz timing reference for synchronization and calibration between the CubeSat and ground station will be obtained from RAFS as baseline signal.

Figure 2.1 : RAFS configuration.

2.2 RAFS Communication Plan

S-band ground station is in the university (UHUZAM) take on the task of communication with the satellite with the appropriate frequency which is 2267 MHZ with 6 MHz bandwidth which the communication concept is defined in Figure 2.2.

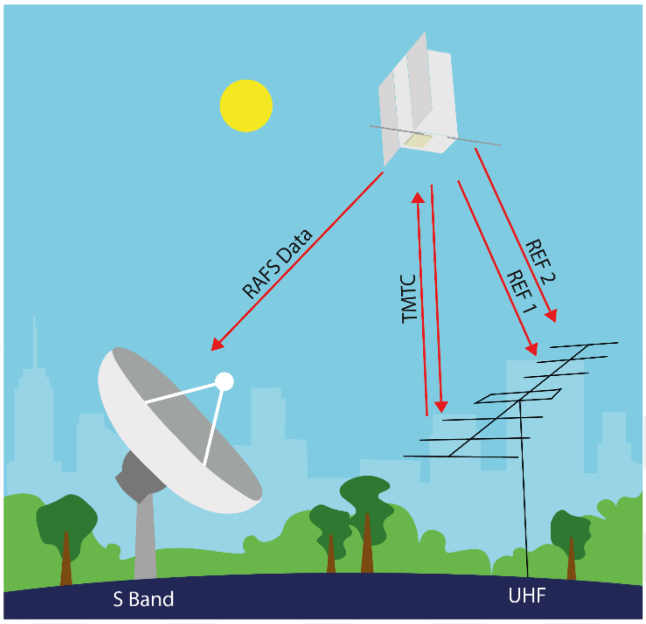

Figure 2.2 : RAFS concept diagram.

2.3 Satellite Communication

2.3.1 Ground station

In this section ground station characteristics and the relationship between said the light and ground station will be investigated. Ground stations are the earth segments of aerospace missions in this case are shown in Figure 2.3 the UHUZAM reflector antenna operates for S-band communication. For this mission and communication with satellite only processes downlink. Satellite communication depends on modems, amplifiers, antennas and low-noise receivers to establish a stable and efficient link between ground stations and spacecraft. It can be optimized with the assistance of suitable modulation techniques, error correction and adaptive transmission for data relay and telemetry.

Figure 2.3 : S-band reflector antenna (UHUZAM).

To establish a reliable exchange of data between satellite and ground stations as S-band satellite communication system, transmitters (TX) and receivers (RX) operate with modems and essential other components. The communication process consists of, with modulation, amplification, and error correction, signal transmission which is known as downlink (from satellite to ground) and signal reception named as uplink (from ground to satellite).

2.3.2 Role of modems in s-band communication

Modems are essential for instant communication, as they fill the gap between data and the radio signals used for transmission, which is modulation and demodulation means converting digital data to RF signals. Modulation encodes digital data (such as telemetry commands) into carrier signals, and the modulation part is relevant for receiving analogue [16]. It extracts the original digital data which should be compatible with modulation. Error correction can be defined in implementation of techniques to improve communication reliability. Encryption provides secure communication for data modulation and adaptive coding altering transmission parameters based on link quality.

2.3.3 Link budget considerations

A link budget aims to calculate and evaluate signal viability by questioning whether communication can be established successfully or not between ground station and satellite in terms of command and telemetry links with defined operational conditions. For instance, the minimum elevation angle scenarios considering power, gain, losses and noise factors.

Key parameters of the CubeSat include 2 MBPS data rate which defines the speed of data transfer, QPSK, 8-PSK, 16-APSK, 32-APS the modulation scheme, 0.5 – 2W transmitter power, LHCP / RHCP polarization. After consideration of link budget, transmission power, gain losses and noise levels should be balanced. Isotropic radiated power (EIRP), bit error rate (BER), and signal-to-noise ratio (SNR) are useful terms to define the communication performance.

2.3.4 Placement of the antenna on the CubeSat constrains, opportunities

Antennas send and receive radiation waves whether they are resonant or non-resonant works efficiently in case of their design and impedance features are tuned to a frequency. The ideal antenna transmitting is one that does not reflect the energy back to the feeding circuit while radiating [3].

Radiation patterns can be categorized as omnidirectional, directional and isotropic. Omnidirectional antennas radiate in all directions with limited gain; directional antennas radiate in a specific direction with higher amount of energy brings higher gain [14]. Therefore, antennas should be specialized according to each mission requirement. Mission requirements and antenna capabilities should be aligned.

For receiving, the ideal antenna design absorbs whole incidence electromagnetic wave without reflection. For fine and continuous communication antenna selection is crucial. In systems using geostationary satellites, since the carrier signal level is quite low, these systems are much more sensitive to noise.

Table 2.1 : IEEE standard letter designations according to their frequency bands [4].

Band Designator	Dimensions
HF	3–30 MHz
VHF	30–300 MHz
UHF	300–3000 MHz
L	1–2 GHz
S	2–4 GHz
Ku	12–18 GHz
Ka	26.5–40 GHz
V	40–75 GHz
W	75–110 GHz

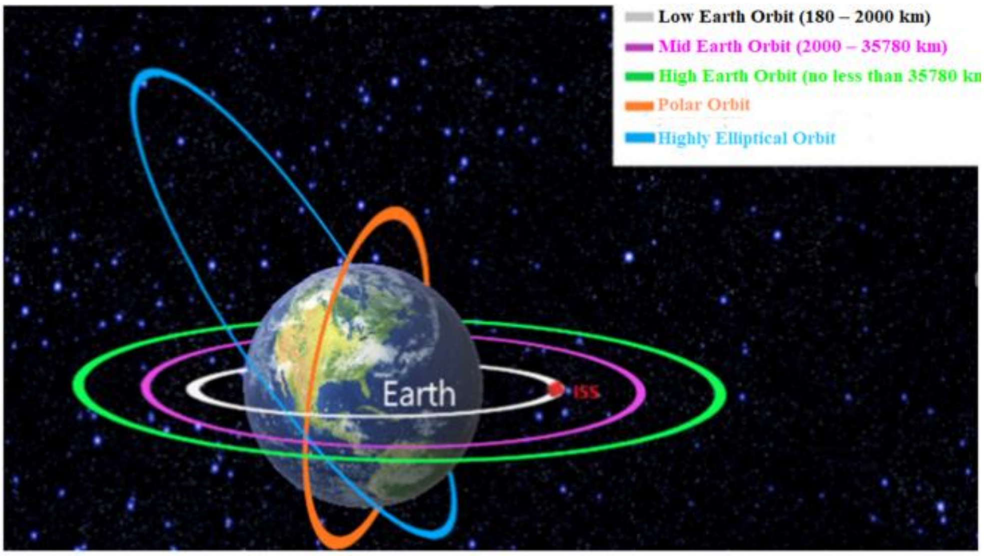

Figure 2.4 : Altitude-classification geocentric orbits.

The popularity of geosynchronous orbit for the launch of satellite systems emerges the advantages of the installation to this orbit which is the coverage of broad geographical area within the orbits demonstrated in Figure 2.4 and frequency bands listed in Table 2.1. Satellites on this orbit can maintain constant communication with the fixed ground station or same satellite which provides no interruptions in communication without any further need for extra tracking systems. The path loss between the ground station is stable for every point within the coverage area. Hence, the satellite which serves a uniform budget and consistent service quality. On the other hand, the Doppler effect on the carrier frequency is negligible. These benefits of geosynchronous orbit facilitate communication operations in terms of both the satellite and the ground station and clarifies frequency management.

2.4 Antenna Selection

The frequency of the mission is defined according to the bandwidth requirement of the communication mission. For S-band is the technique for higher bandwidth selection, which is made according to the mission for CubeSats for primary uplink and downlink. Monopole and dipole antennas, which can make 12 band operations, can be used for transmitting and receiving data at the same time and they mostly require deployment mechanisms with type string.

Antennas are necessarily utilized spacecrafts, and they operate in specific frequency bands. The second popular Patch planar antennas which are easy to assemble can provide constable gain compared to monopoles and dipoles don't provide circular polarization and high gain. Also, patch antennas can be used for higher data rate communications telemetries. Helical antennas, another candidate useful for CubeSat missions for observatory observations.

Directive antennas can be designed to be deployable, enabling compact storage and rapid deployment in space applications. High-speed communication demands have led to the development of various antenna types, including optical (light) communication links and antennas tailored for low Earth orbit missions. Additionally, guided-wave antennas have become prominent choices for frequency bands such as Ka-band and V-band. Over time, these diverse antenna technologies have emerged, evolved, and become widely used. However, in the early days of antenna design, only simple monopole and dipole antenna types were considered. In Figure 2.5, there is the graph for the comparison provided gain level.

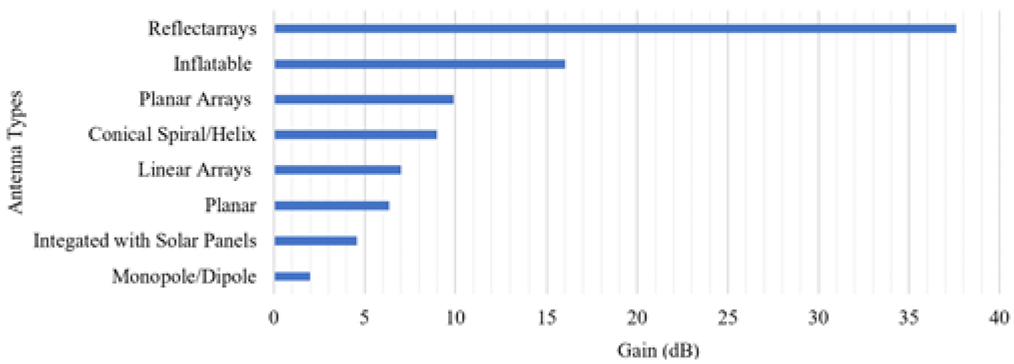

Figure 2.5 : Antenna types according to gain level.

From the study results gathered from 120 CubeSat operations between the years 2003 to 2022 with various missions to analyze different antenna types and their behavior related to operating frequencies as can be seen in Figure 2.7. According to the data taken from the study proves following array antennas (multi-element antennas) and inflatable antennas, helical antennas provide the highest values with approximately 9 dB which makes helical antennas are well-matched antennas for Earth observation communication and IoT missions. As seen in Figure 2.6, within single and single-element antennas, helical antennas promise the highest gain potential [4].

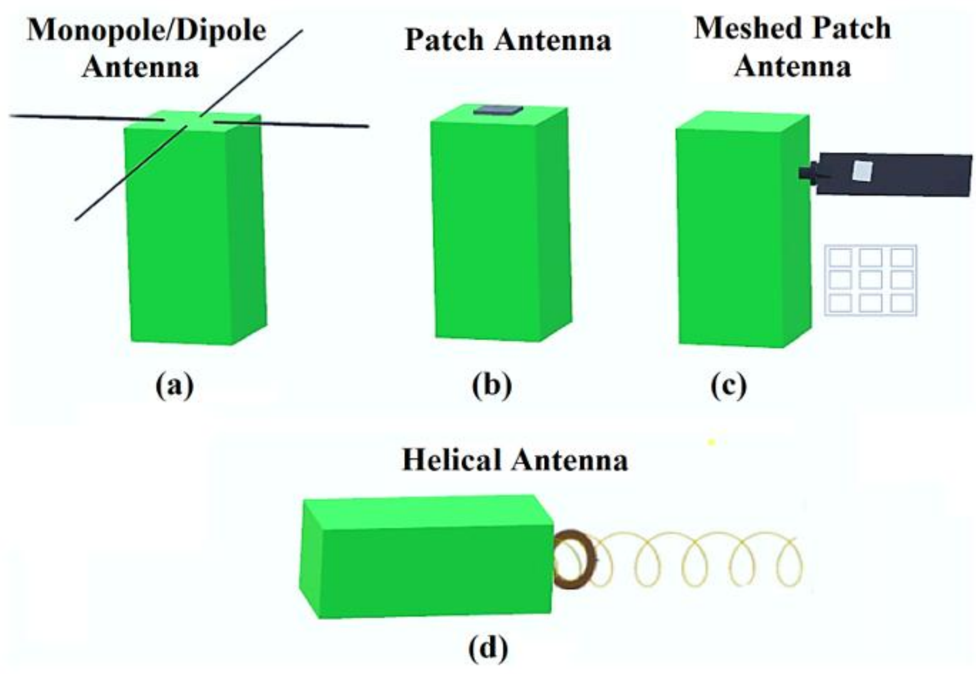

Figure 2.6 : Common antenna types (a) monopole/ dipole antenna (b) patch antenna (c) meshed patch antenna (d) helical antenna.

Communication systems should be suitable for both fixed and mobile applications. Fixed satellite terminals do not require a very wide beamwidth or low gain for proper operation. However, mobile applications require antennas with moderate beamwidth and lower gain due to movement, making their installation and maintenance easier. Such applications prefer low-gain antennas with wider beamwidths to ensure continuous connectivity despite movement. However, because these antennas have lower gain, their efficiency is reduced.

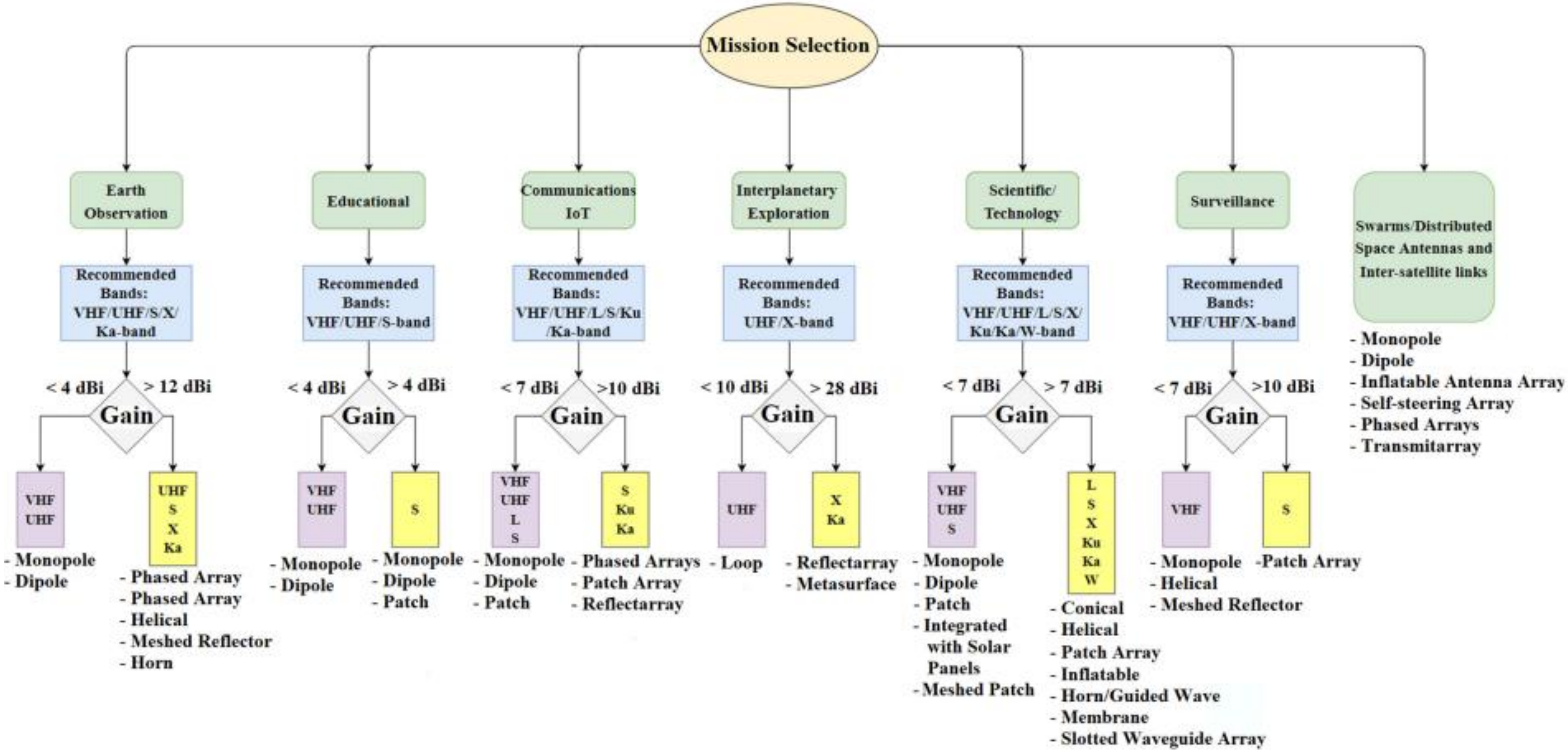

Figure 2.7 : Antenna selection according to missions [4].

Table 2.2 : Comparison of comprehensive antenna types and characteristics.

Type	Bands	Characteristics	Advantages	Challenges	Applications
Monopole & Dipole	VHF (30-300 MHz), UHF (300-1000 MHz)	Simple, omni-directional radiation pattern, compact.	Low cost, easy to deploy, suitable for basic telemetry.	Limited gain, deployment risks	Low data-rate telemetry, basic communication.
Helical Antennas	UHF, S-band (2-4 GHz)	Circular polarization, compact (stowed), medium directivity.	Compact, lightweight, no deployment needed, higher gain.	More complex design and integration.	Inter-satellite links, moderate communication.
Phased Arrays	X-band (8-12 GHz), Ka-band (26-40 GHz)	Multiple radiating elements, electronically steerable beams.	Good gain-to-size ratio, ideal for moderate data rates.	High cost, power-hungry, complex to design.	IoT, 5G, inter-satellite links, deep-space communication.
Reflect arrays	Ka-band, W-band (75-110 GHz)	High gain, large aperture, directional.	Excellent for high-data-rate links, long-distance comms.	Bulky, heavy, needs precise alignment.	Deep-space communication, high-res observation.
Parabolic Reflectors	X-band, Ka-band	High gain, parabolic shape	Very high gain ideal	Size, weight, complex	Deep-space and planetary

Deployable helical antennas are considered as main candidate for CubeSat communication applications due to their broad bandwidth of operation as well as their natural circular polarization behavior. Another candidate for CubeSat operation is the quadrifilar helix antenna which can be either shorted or open at the top of its conductors. This antenna structure exhibits a reasonable bandwidth. Patch antennas have also been proposed as candidates which can be printed on one of the satellite surfaces. These antennas also can exhibit circular polarization and adequate bandwidth. However, their operation in a S-band cannot provide high level gain as compared to helical and quadrifilar antennas [33]. In Table 2.2, there is a detailed comparison between antenna types and their characteristics.

2.5 Literature Review

Helical antennas which exhibit 360-degree azimuth beam pattern offers natural circular polarization with raised bandwidth and gain compared to monopole and dipole antennas. This radiation pattern characteristics define helical antennas. The elevation of the beam, which is defined by beamwidth pattern, can be modified by changing the axial antenna height as a function of wavelength which exhibits a higher gain at designated elevation angles. The Iso-flux antenna beam radiation pattern makes helical antennas an attractive option for CubeSat missions attempted at receiving low-power signals transmitted at low elevation angles, which are often difficult to capture using ground stations [17]. The advantage of achieving high gain at low elevation angles like LEO orbit provides the satellite to consist of it is not the pointing while receiving radio frequency energy from ground station which is terrestrial emitters. There is a comparison between the types of helical antennas in terms of RF characteristics in Table 2.3.

Table 2.3 : Performance of conical spiral and helical antennas [4].

Type of the Antenna	Frequency (GHz)	Gain	-10 Db BW (MHz)	Deployable
Helical	0.400	13	N/A	Yes
Hemispherical Helical	2.45	13.2	N/A	Yes
Bottom-Fed	2.2-3.1	11.2	900	Yes
Conical	0.300-0.600	5	300	Yes
Quadrifilar Helix	0.250-0.500	5.41	Various	Yes

The gain of helical antennas which can have turn number between 5 and 15 operating changes according to the number of turns at axial mode. Especially, the gain enhances as the number of turns increases. Although it is a known fact the gain increases as the number of turns increases, which is not linearly according to the simulation as pointed out at figure 2.8. After 10 turns the enhancement of gain does not observe, there is no notable change in the gain level, and it does not necessarily result in a more directional radiation pattern [43].

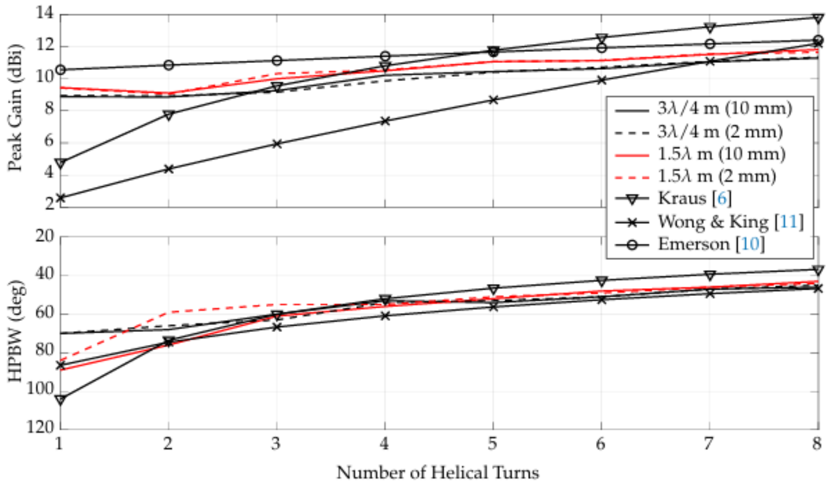

Figure 2.8 : Relationship between number of turns and gain – HPBW.

Table 2.4 : Simulated gain comparison according to number of turns of the bifilar skeleton SHA.

Number of Turns	2	4	6	8	10
Hexagon SHA Gain (dBi)	9.94	11.5	13.23	14	14.38
Square SHA Gain (dBi)	9.85	11.27	12.85	13.64	14.04

Table 2.4 shows the comparison between the variation of the simulated gain and the number of turns of bifilar structure SHAs. From the outcome, these are obtained also, higher gain can be achieved by adding reactors or helical antenna arrays.

2.5.1 Other Satellites and Their Antennas

2.5.1.1 GOMX-1 and GOMX-3 missions

Both GOMX-1 and GOMX-3 missions shown in Figure 2.9 utilized commercial helical antennas as payload antennas for Automatic Dependent Surveillance-Broadcast (ADS-B) data acquisition [7]. These antennas were stowed within the satellite during launch and deployed once in orbit, demonstrating the feasibility of using helical antennas in CubeSat platforms. Gomx-1 is a satellite which can track trans ocean flights with the help of reception of the Automatic Dependent Surveillance-Broadcast signal as summarized in Figure 2.10. Mission is traffic control. It is launched at in November 2012. Helical antennas gain is 10 dB at 1090 MHz. For ADS-B data acquisition high gain and high directivity are necessary parameters. Other options are arrays as single element antenna helical antennas are used.

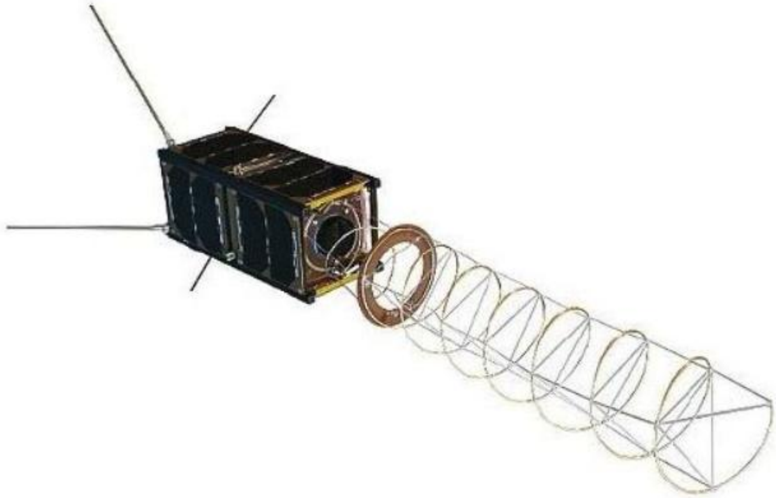

Figure 2.9 : GOMX-1 with deployed antennas.

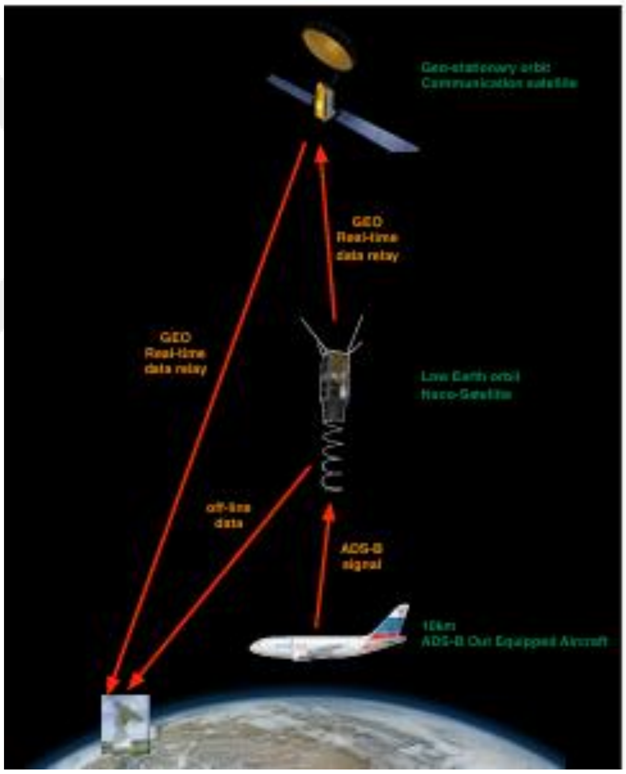

Figure 2.10 : ADS-B mission concept design.

2.5.1.2 Lacuna space IoT missions

Lacuna Space launched CubeSats in Figure 2.11 and with helical antennas assigned for Internet of Things (IoT) applications mission [29]. Operating in the UHF LoRa frequency bands, these deployable antennas enable reliable communication with ground-based IoT devices, showcasing the versatility of helical antennas in supporting IoT connectivity from space.

Figure 2.11 : Lacuna space configuration.

2.5.1.3 CubeRRT mission

The CubeSat Radiometer Radio Frequency Interference Technology Validation (CubeRRT) project visualized in Figure 2.12 determines a particular digital based spectrometer qualified for special algorithms that can define and mitigate the radio interference. Corroborated with circular polarization, the CubeSats antenna structure system is in the structure of a dual helical configuration capable of tuning across the 6–40 GHz frequency band. The whole project belongs to the Ohio State University. The highest gain the system reaches is 12 dBi at 6 GHz and 21 dBi at 40 GHz. The mission clarifies the effectiveness of helical antennas which are continuous taper in wideband antenna system CubeSat applications based on their flexible geometry, wide bandwidth, wide bandwidth and simple feeding mechanism and circular polarization [32].

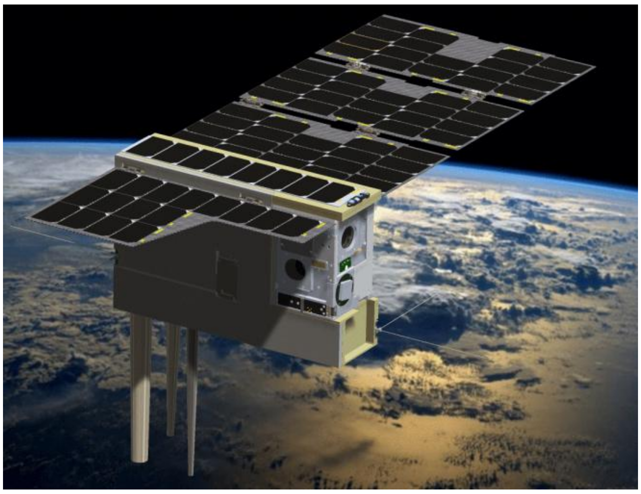

Figure 2.12 : CubeRRT.

2.5.1.4 HCT QHA

In the CubeSat deployable QHA project developed and run by Kellogg's Research Lab, a HCT antenna's fundamental components are shape memory alloy (SMA) antenna filars, a milled ULTEM casing, electronics board and SMA hold and release structure. The hold downs provide to keep the system stowed during launch in the deployer and following initial operations. The SMA antenna filars shown in Figure 2.13 do not activate their deployment configuration until sufficient power is applied to hold-downs but they still possess enough strain energy to extend and protrude from the antenna casing. Nitinol which is an ally consisting of Titanium and Nickel is commonly used SMA metal for spacecraft deployment mechanisms also used in this project in both filars and hold-down elements of HCT shown in Figure 2.14. The system works as an electrical current which flows though the circuit turns into heat and it increases the temperature at the intersect point until the alloy changes and becomes necessary shape which alloys the mechanism to supply deployment excitation movement [16].

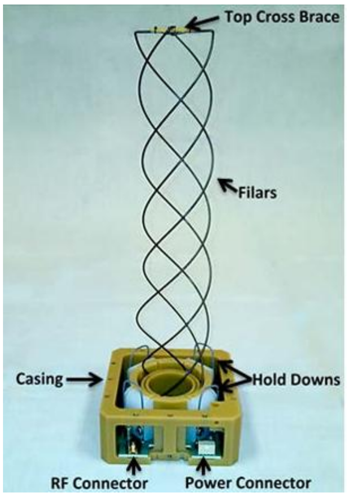

Figure 2.13 : HCT QHA deployment mechanism components.

Figure 2.14 : HCT QHA hold down and release mechanism.

To summarize the SMA deployment mechanism, the required voltage and temperature are calculated to realize the deployment and maintain the deployed version of the geometry even after voltage is removed. (Testing the deployment on earth deploying the antenna upwards which is against gravity and on the opposite deploying downwards on the behalf of gravity. They affect the deformations differently than the space. In space there are no geometrical deformations like drooping, it should be considered during testing in gravity.

2.5.1.5 Cat-4 mission

The Cat-4 missions shown in Figure 2.16 combines GNSS-R and Microwave Radiometer payload into a 1-Unit CubeSat aimed to demonstrate Earth Observation capabilities by integrating them. A significant challenge was designing a deployable helical antenna that fit within the 1-Unit. Main reason of this challenge is the expectation for the improvement on current earth observations which hold-down mechanism shown in Figure 2.15.

Thanks to the helical antenna capabilities, the CubeSat can switch frequency bands because of the feature of gradual deploying in the GPS. In L1 mode antenna operates in 1575 MHz, while it is shorter because of the gradual deployment it shifts to L2 mode the frequency moves to 1227 Mhz and the microwave radiometry band (1400–1427 MHz). The adjustability of helical antenna designs in multi-frequency applications is emphasized in project [18].

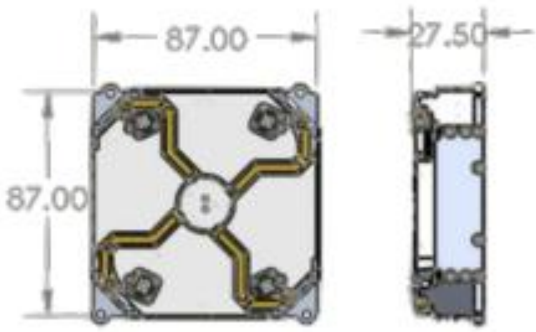

Figure 2.15 : Hold-down folder fingers.

Figure 2.16 : Deployed configuration of 1U Cubesat Cat-4.

2.5.1.6 Skynet mission

UK's Skynet Satellites, which are four satellites, built to the Stage 2 standard (Skynet 4d, 4e, 4f) incorporated helical antennas especially in the Skynet 4 series visualized in Figure 2.17. The purpose of these antennas is to prove holistic Earth coverage, promote security and to offer reliable Earth-cover UHF communication mission efficiently for military operations. For deployment mechanism, brass fingers and dyneema wire is locked in the center of antenna, after it is deployed with the power of resistance antenna becomes the highest potential configuration. [21]

Figure 2.17 : Skynet configuration.

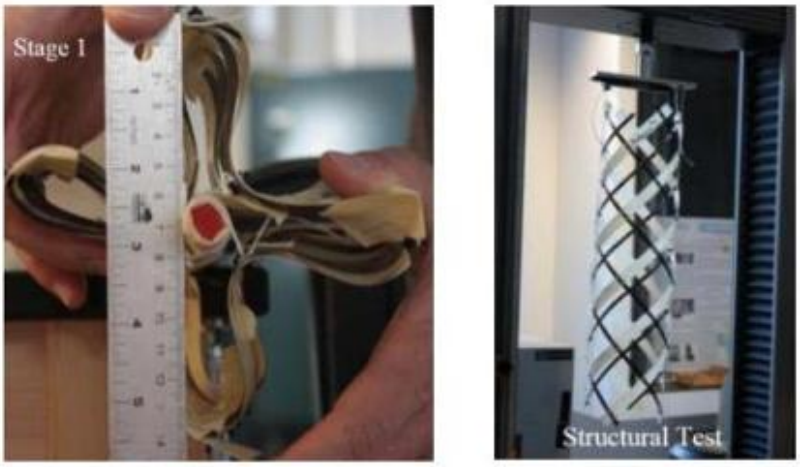

(a) (b)

Figure 2.18 : Deployable helical antenna a) fully stowed b) fully deployed.

Another academic study is conducted by J. Costantine, Y. Tawk, I. Maqueda, M. Sakovsky, G. Olson, S. Pellegrino, C. G. Christodoulou. The antenna's deployable and in the structure of quadrifilar shown in Figure 2.18. Antenna consists of four conductive arms which is the material beryllium arms and nonconductive hinges at connection points to have directive behavior it has a ground plane. to reduce the back lobe in the radiation, pattern the ground plane diameter is raised [10]. The system provides %7.12 bandwidth, -27 dB reflection coefficient and 8.38 dbi total gain.

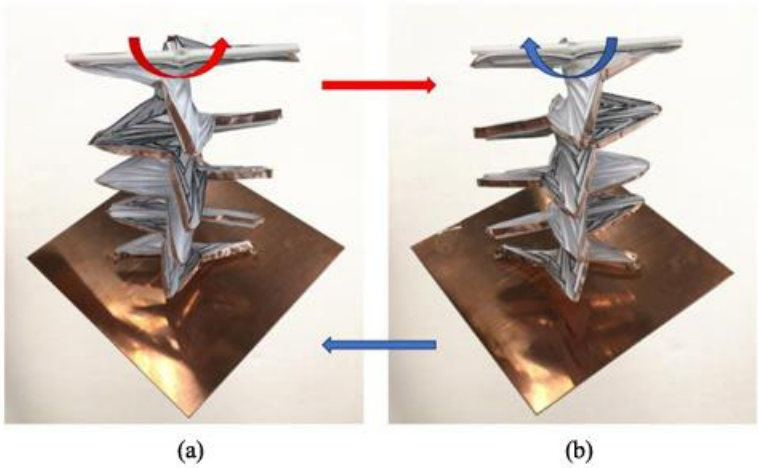

Figure 2.19 : The manufactured prototype of origami SHA at (a) LHCP and (b) RHCP.

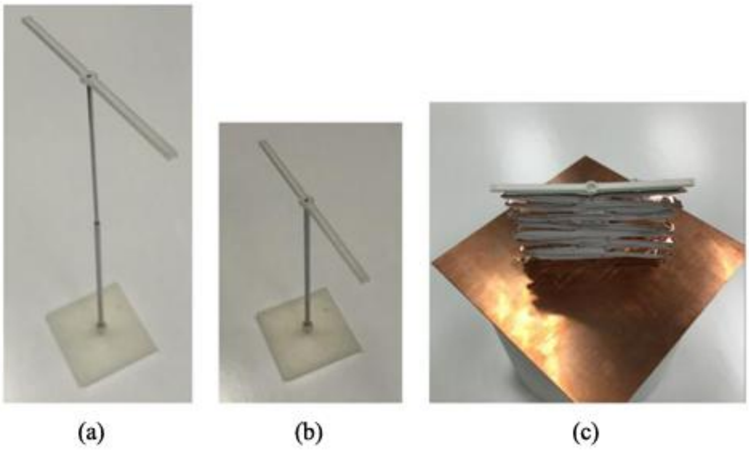

Figure 2.20 : (a) Expanded telescoping central axis, (b) collapsed telescoping central axis (c) tightly folded origami SHA.

The structure platform shown in figure 2.21 can be rotated around its central axis by twisting the PLA arm. The feeding mechanism can be summarized as antenna's copper wire is connected at the ground plate of the antenna to a 50 Ohm excitation and the other end of each copper wire is fixed to the highest point on the arm which means ports for two excitations have 180 phase differences between them shown in Figures 2.19 and 2.20 [48].

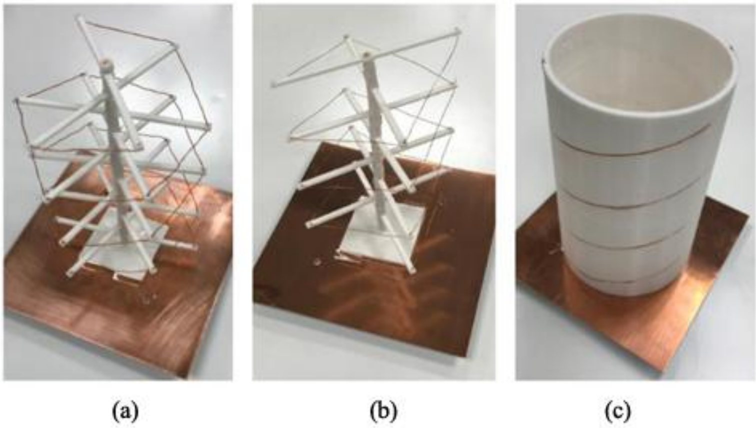

Figure 2.21 : Fabricated mockup of the (a) hexagon structure SHA, (b) square skeleton SHA, and (c) conventional HA.

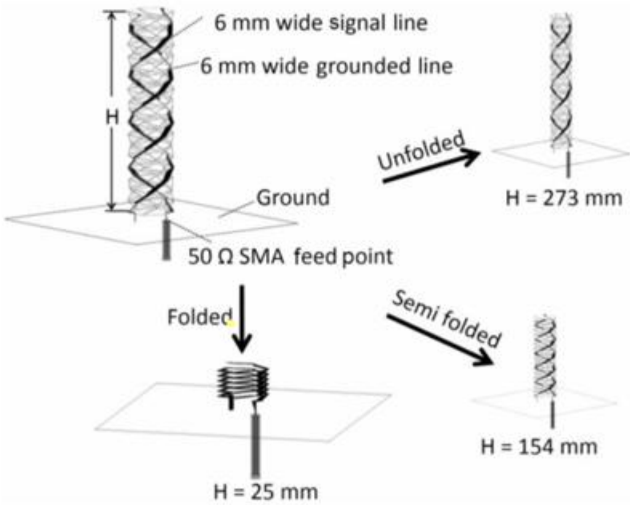

Figure 2.22 : Bifilar foil structured origami helical antenna.

Another study on origami structured helical antenna shown in Figure 2.22 aimed to change operating frequency by changing the height. This antenna was constructed using 0.1 mm thick copper tape on a 0.2 mm thick sketching paper substrate, without any additional coating. The copper tape was glued to the paper and folded together with it, ensuring that it remained attached to the paper base during both folded and unfolded state [43].

2.6 Deployment Mechanism

Motors and active actuators are not considered in the process because they require extra energy and more space although it has its continuous velocity potential [35]. From the system and executing a proper antenna in this way is a more complex process, especially for a small satellite and its antenna [19]. The innovation in this study is the integration of burn wire systems and deployment axial movement. Presenting a deployment system which is less like a conductive foil but the original wire antenna. Since the helix behaves like spring, the reason is spring geometric structure and its stored elastic potential energy turning into kinetic energy the releasing of antenna deploys antenna naturally. Maintaining the exact values defined in the design parameters is critical to ensuring proper antenna performance. Each Kresling cell is designed to function as a hinge, facilitating the desired folding and deployment behavior of the structure. The Origami is wrapped around the antenna will be a tensioned structure. With a pattern of holes is defined as a guide which gives the antenna its calculated shape.

In this section selected materials, which is Kapton® 300 HN polyimide film some mechanical and thermal characteristics are explained. Kapton® 300 HN polyimide film has a nominal thickness of 0.08 mm, a density of approximately 1.42 g/cm^3, and an operational temperature is an extensive range from −269 °C to +400 °C which makes the material convenient match for space applications [40].

The mechanical aspect of material properties is also remarkable. Its tensile strength is around 231 Mpa, exhibits excellent mechanical strength additionally with elongation at break of 72% provides durability during deployment. Calculations and tests show for a 1-meter-wide strip with 0.08 mm thickness; the expected breaking force is approximately 18,480 N [3]. This clearly proves that polyamide film is highly sufficient to withstand the sudden mechanical loads, offering a safety margin thousands of times greater than the 0.3 N force exerted by the antenna's deployment structure. Under static conditions to protect the pitch angle and spacing between turns preserved as the origami structure, polyamide Kapton which is a stiff material is suitable.

Deployment mechanisms for space applications can be categorized since it is an open for improvement topic and NASA included so many labs trying to develop new designs and configurations [47]. To make sure the antenna deploys safely all the elements should be considered step by step and accurately. These two dependable previously tested and executed systems were on the consideration. The practical and low-cost versions of these studies were desired.

According to the literature, wire-burn deployment systems typically consist of cover and hinge mechanisms such as two outward-directional opening lids or a single lid with brass fingers that release after activation to enable deployment. Additionally, some designs incorporate shape memory alloys, which are activated by high temperatures to allow antenna deployment.

A crucial component for releasing the hold-down mechanism or also to hold it involves tied knot and restrained wire which has been used for secure and durable systems. Knot component must resist vibration, unexpected forces and mechanical stresses. The tension must not be loosened because it could jeopardize the deployment itself. It is an extremely critical approach to actuator; at the same time, it is simpler and feasible compared the other systems like shape memory alloys. With repetitive testing the engineers must make sure the system is dependable before considering space launch [4].

2.6.1 Advanced deployable structural systems for small satellites

In this section some of the existing deployment technologies and studies are examined. These systems are crucial components for enabling limited volume spacecraft like CubeSats for adapting them to be functional for components like solar arrays communication antennas sensors and drag sails. These deployment mechanisms should be implemented.

The aim is to improve deployable boom performance consistency and feasibility on the ground, integrate designs that have tolerance for production variances and associate with functionally reliable and straight forward deployment systems. Since CubeSats are small and packed spacecrafts it is requested to have dependable and membrane deployment concepts [44]. Narrowing down existing deployable mechanism solutions for CubeSats causes manufacturing problems, the reason why limited compact stowing volume. Since, State of the art spacecraft boom concepts are designed for large satellites with large appendages. Therefore, structures for CubeSat systems should be specifically designed by considering necessity and limitations [33].

Currently, there should be increasing numbers of efficient boom and membrane deployment concepts which have lots of use for small satellites. Each of them is crucial for topics like communication, power generation and data collection.

The main boom configurations utilized in space deployment systems consist of storable, extendable tubular member (STEM), truss shown in the 2.25, telescopic and mini-collapsible tubular mast (mini-CTM or Omega) booms [23]. Other considerable kinds of booms are rollable collapsible (TRAC) seen in the figure 2.28 and triangular, low-stiction polymer tube (shearless) and sheath-based rollable lenticular-shaped booms. For the International Space Station (ISS) configuration in Figure 2.23, eight FAST-Masts (see Figure 2.24) are implemented to facilitate the deployment of solar arrays.

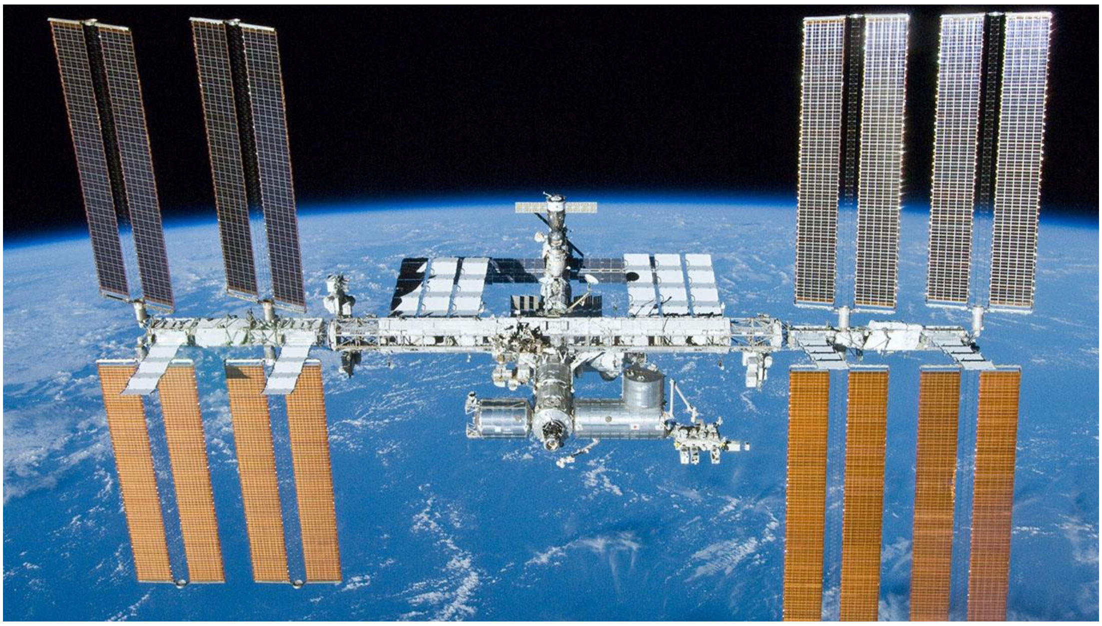

Figure 2.23 : International Space Station (ISS).

Prototyped supports are also used with 3D printers. A prototype of the system was constructed from 3D printed structural components, as well as purchased bearings and motors, and flexure springs cut from tempered 301 steel sheets.

2.6.2 Truss booms

Truss booms have high strength and stiffness and reliable and efficient systems and the type of deployment is planned as a balanced structure element like geometry stiffness, mechanical stability and strength. Mechanism works as a packed structure becomes reliably expanded [28].

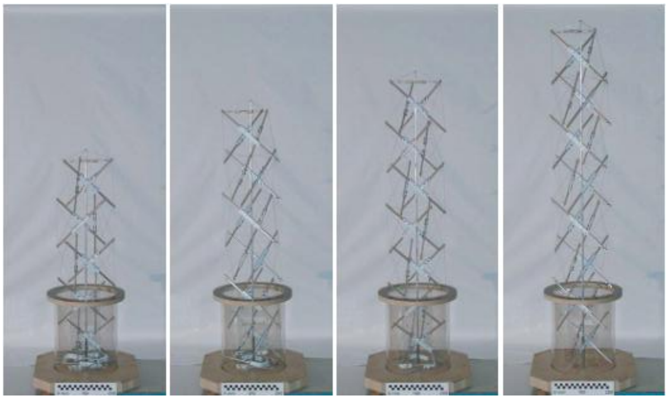

Figure 2.24 : Rod-controlled deployment steps.

Fig. 11: Beginning deployment of ADAMmast (Source: NASA)

Fig. 12: Deployed FAST mast as used on ISS (Courtesy of Able Engineering – Extracted from [7])

Fig. 13: FAST mast deployment Principle(Extracted from [7])

Figure 2.25 : Truss boom deployment principle.

The satellite named Aeneas visualized in Figure 2.27 has a telescopic type of antenna configuration. In Figure 2.26, it is seen a spring-loaded hinge joint [45]. During deployment, rib slides upward while the telescoping waveguide does not move. The connection of the inner and outer portions provides deployment.

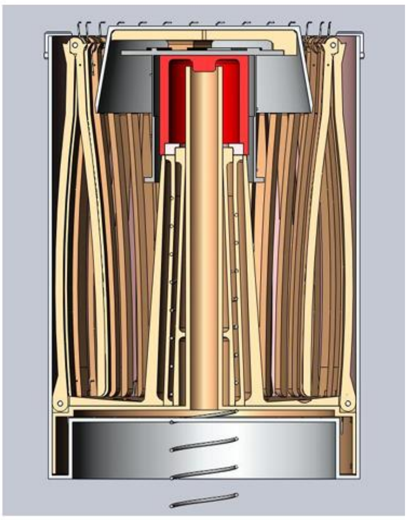

Figure 2.26 : Telescopic mechanism.

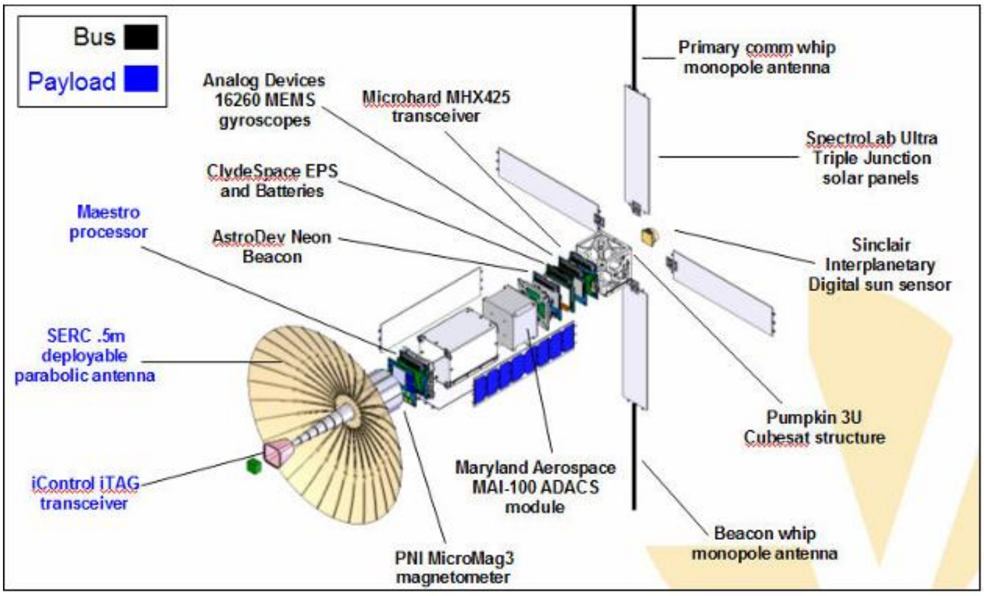

Figure 2.27 : Antenna and satellite configuration [43].

2.6.3 Rollable and collapsible booms

For this configuration deployable thin shell composite booms are used. Booms are flattened when they are stowed once they get free composites become their original shape and this provides a deployed structure to hold payload shown in Figure 2.29 and solar sail configuration visualized in Figure 2.30 [49].

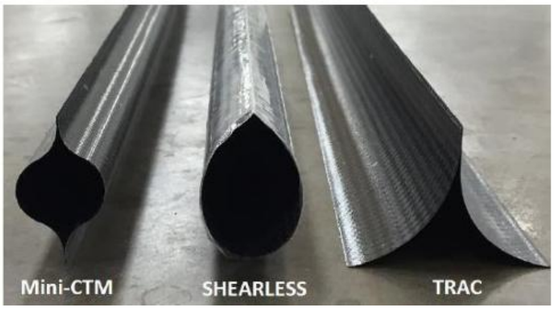

Figure 2.28 : Boom geometries.

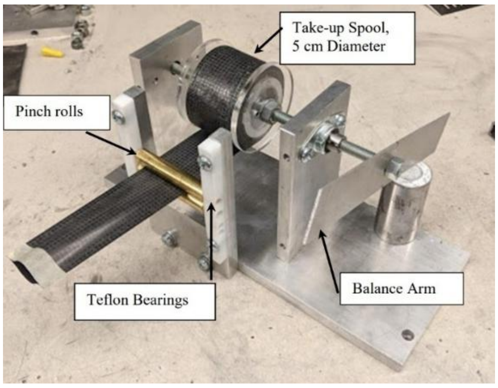

Figure 2.29 : Rollable boom mechanism.

Since these considered mechanisms are so complicated, I conveyed simpler solutions for deployment and elongation of mechanisms. Consequently, antenna length is determined by operating frequency and by folding and unfolding the origami-based geometry, changes the operating frequency by the length extension or shortening. Frequency tuning can be achieved by arranging structural. Unlike typical antennas applying λ\2 or λ\4 resonance, the origami helical antenna shows variations in resonance frequency depending on its state. In stowed state the origami helical antenna resonance frequency increases and when it is deployed the resonant frequency of the helical origami antenna decreases [29].

After comparing the mechanisms mentioned, evaluating constraints and opportunities in the orbit and considering the scale of the project, the decision is made to move forward with the origami structure. Therefore, origami structures are feasible, easy to fabricate and functionally acceptable and controllable.

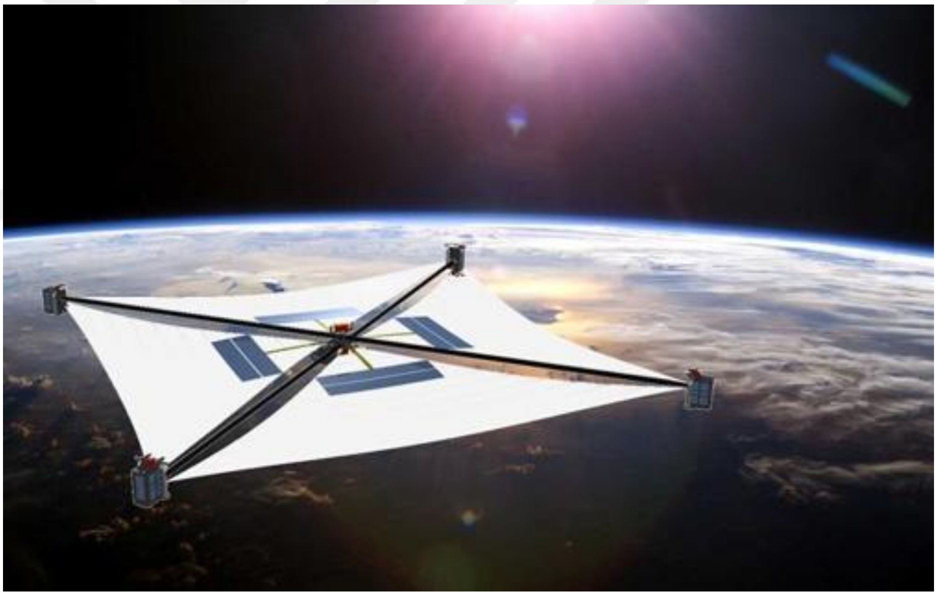

Figure 2.30 : GOSSAMER-1 solar sail developed by DLR.

2.6.4 Origami

Origami to define simply patterned sheets of material to alter the patterned sheets into engineering mechanisms, so many techniques can be used. For instance, many parts can be produced separately and attached which might have so many borduns and risks. The other choice can be crafting one piece of material without any cutting and separation. Test mockups is folded manually but to minimize the failure of the sheet can be obtained by automatized systems like laser machines. This way, motion providing Kreslings can be applied on the surface of sheet as assigned folds. The usage of folding sheets to pattered 3D configurations, which is the basis of origami is the traditional and ancient Japanese art of their culture gifted to global society. Recently, the potential of origami has been discovered in the technical literature in also space industry on solar panels antenna systems payloads it can be used in near future even for civilization on other planets projects. For the design, it is detailly searched for suitable origami design to provide and create a system that works in harmony with rest of the system and antenna.

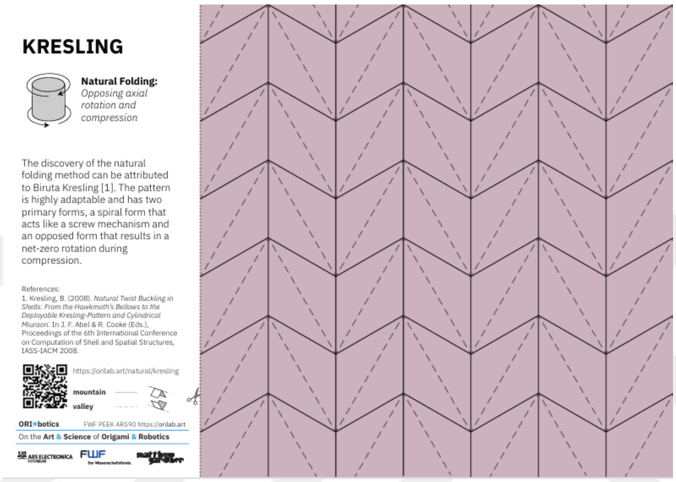

Figure 2.31 : Kresling drawing.

Kresling Natural Folding method which is shown in Figure 2.31 is the match for the project which has the features of opposing axial rotation and compression without getting broader on the x axis which refers to no transform in the diameter, only axial force. The discovery of the natural folding method can be attributed to Biruta Kresling a implemented version for the necessary geometry [36]. The pattern is easily adjustable and based on two main mechanisms, the first one is a spiral form that behaves as screw mechanism and second one is an opposed form that results with no rotational movement while bringing the linear compression.

Castigliano's theorem is a fundamental principle in structural mechanics used to calculate deflections or forces in elastic systems. According to this theorem, the force F_a acting at a particular point in a structure can be determined by taking the partial derivative of the total strain energy U of the system with respect to the displacement h at that point. Mathematically, this relationship is expressed as,

$$F_a = \frac{\partial U}{\partial h} \tag{2.1}$$

According to Castigiano's theorem, bending and twisting of structure changes the stored strain energy of the structure thanks to the elastic deformation of the mechanism. The outcome of the stored strain energy acts along the axis of the helical antenna. The minimum potential energy regions where the restoring forces equal to zero (Fa=0) are the stable points of the structure which transforms the structure towards its minimum energy configuration which means setting the equilibrium form. Therefore, the structure can sustain the movement without external power. When the radiuses are pushed to max and min position, there are extra stable points at these limits [31].

It is encouraged to develop systems that enable low-energy, user-centric reconfiguration of structures without the need for DC motor actuators. The use of fiber-reinforced polymer composites (FRP) as the strip material has been demonstrated to significantly enhance structural stability. This material choice, due to its favorable mechanical properties, offers a wide spectrum of design possibilities and has been proven effective in numerous studies [36].

Origami systems are not irrelevant to space applications. It is common for configurations like solar panels, telescope structures and antennas which are a research area open for more development. It is demonstrated in Figure 2.32, the James Webb telescope which is the mechanism based on origami.

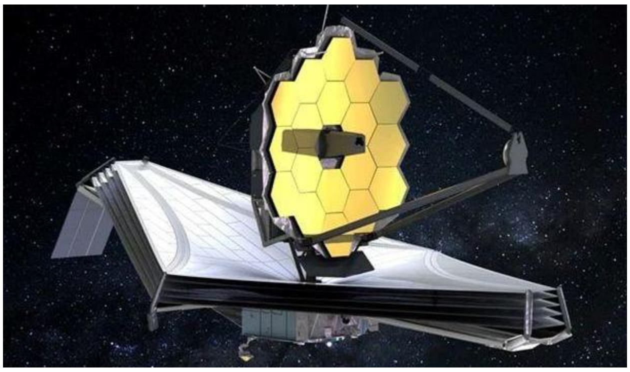

Figure 2.32 : The James Webb telescope.

2.6.4.1 Kinematics of origami

A similar study examines the geometrical behavior of the axial movement of origami structure which assisted to comprehend the math of structure.

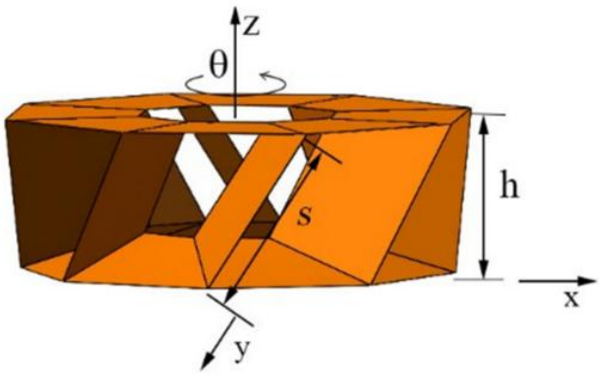

Figure 2.33 : Schematics of axial motion with rotation angle.

As the vertical height (distance between the top and bottom plates) h, rotation angle around the z-axis, s length of the diagonal link plate as visualized in figure 2.31. The relationship is regulated by the geometry of the Kresling mechanism and is explained by the given equation [20].

A function of rotation (height),

$$h = s\sqrt{\left(1 - \frac{sin^2(\theta/2)}{sin^2(\pi/8)}\right)} \tag{2.2}$$

The length of the link plate length s,

$$s = L - Lsin(\pi/8) \tag{2.3}$$

height without rotation, Twisting leads to the axial extension (construction) without bending in case the top plates stay parallel and aligned.

$$H_0 \; = \; s = L - Lsin(\pi/8) \tag{2.4}$$

In the context of the origami-based structure, h denotes the instantaneous vertical height between the top and bottom plates, representing the current compressed or extended state of the system. The parameter s corresponds to the length of the diagonal creased link (or link plate) that connects the edges of the polygonal faces, playing a critical role in determining the overall kinematics of the fold. The angle θ describes the in-plane rotation around the z-axis, capturing the twisting behavior of the structure during deployment or compression. Lastly, L represents half of the total length of the origami structure when fully unfolded, serving as a key geometric reference in evaluating the deployed configuration [26].

The graphic demonstrates a deformable origami structure where the height between the top and bottom plates alters the structure twisting around the z axis by Theta angle.

3. ANTENNA DESIGN

3.1 Characteristics of the Antenna Wire

S11 values are simulated and compared in HFSS software to decide the characteristics of the antenna such as total and axial length, pitch angle, diameter of antenna. The plot at Figure 3.1 demonstrates the S11 diagram (return loss) of a variety of antenna configurations created by different design parameters. It was searched for the highest RF efficiency, changing the total length, spacing between turns and the number of turns. It is aimed at reaching the smallest return loss while converging to the center frequency which is 2267 MHz. Diameter dimensions differ between 40-50 mm and total length difference between 120 mm and 240 mm. Spacing between turns changes between 19 mm and 37.1 mm. Lines represent their reflection coefficients across a defined frequency range. The smallest values on this graph are the proof of a strong resonance and less reflected radiation [13].

The antenna must be well-balanced between the terms of frequency and efficiency. Although the lowest reflection coefficient (return loss) reached around –50 dB, but it does not between the required frequency range, it does not accomplish the goal. In some parts of the frequency spectrum, the reflection coefficient was even higher than 0 dB, which is undesirable these configurations were eliminated. The goal of this analysis was to achieve a return loss of approximately –30 dB at the desired frequency.

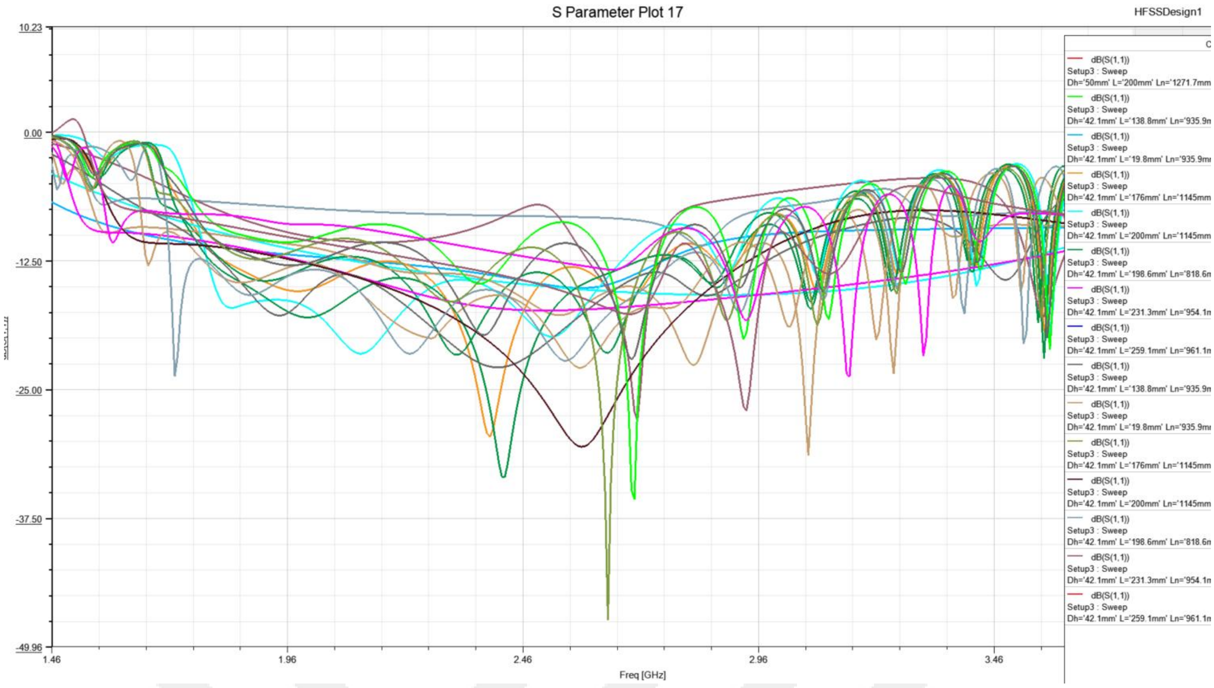

Figure 3.1 : S11 return loss plot.

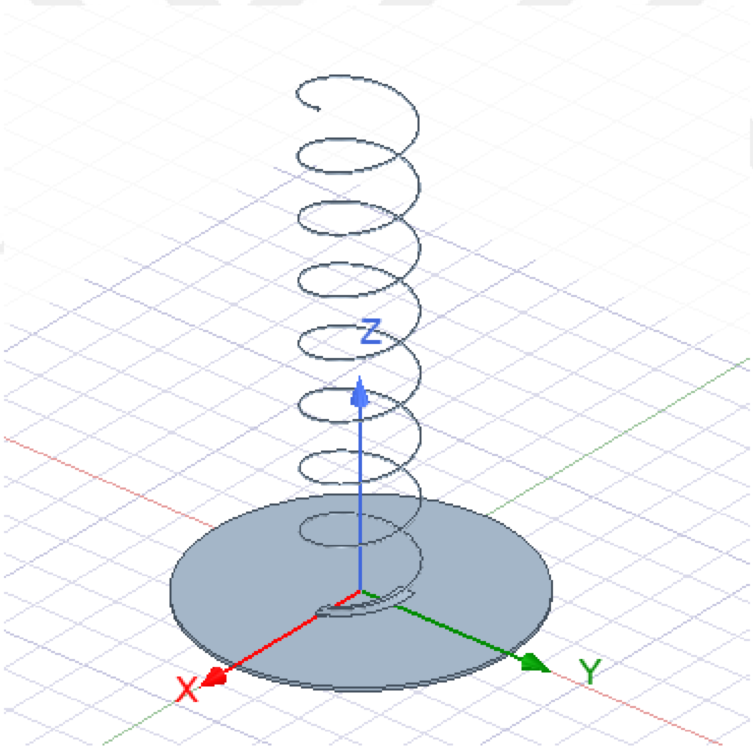

Figure 3.2 : HFSS model of helical antenna.

The model shown in Figure 3.2 and Table 3.1 is the configuration is selected as final design configuration because these values are the most optimized which refers to the required frequency value and low return loss.

Table 3.1 : Design parameters.

Parameter	Value
Wire Material	Silver coated aluminum
Ground Plane Material	Aluminum
Feed Material	Copper
Diameter of ground plane, mm	100
Spacing between each turn, mm	22.2
Total length of antenna, mm	176
Number of turns	8
Helix Diameter, mm	42.1
Circumference of helix	132.3
Length of coaxial feed, mm	10
Thickness of ground plane, mm	2
Distance between feed and helix, mm	2
Total Length of Wire, mm	954.1

After obtaining the HFSS simulation results with mentioned design parameters with slight differences which demonstrate that the antenna configurations operate in the s-band between 1.75-2.50 GHz (see Figure 3.3), fine frequency tuning was performed using a spectrum analyzer (see Section 5).

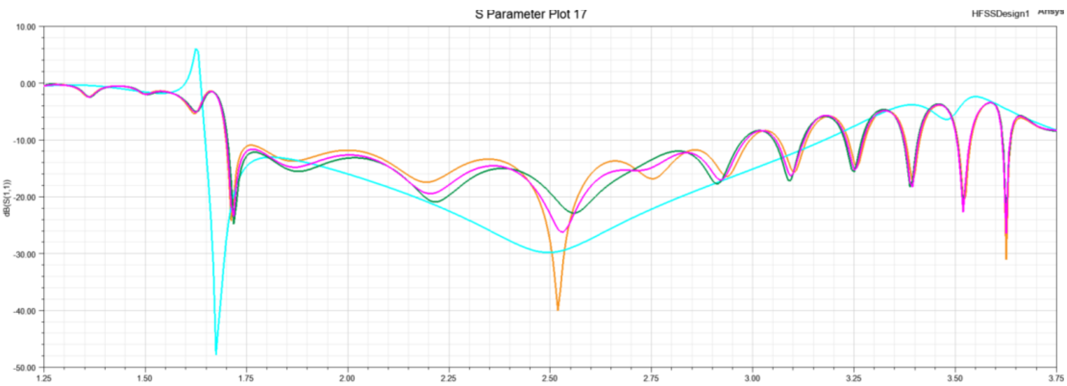

Figure 3.3 : HFSS simulation results in s-band.

3.2 Wire Design

By aiming the circular polarization and directionality high gain, it is approached to enhance 6U CubeSat communication to transfer more amount of data reliably in S-band. For the antenna analyzed using ANSYS HFSS, by using parametric sweeps performed to optimize its radiation performance in terms of gain, efficiency, axial ratio. Wire design is conducted with results that come from the analysis because the efficiency of the wire is defined with facts of antenna calculations and analysis. Antenna characteristics are obtained by antenna theory calculations.

3.3 Comparison of Number of Turns

With 7 turns the efficiency of antenna increases, in terms of measurements 6 turns also analyzed to observe how it works. But with 7 turns antenna gave more sharp reflections compared to 6 turns. At the latest simulations, the outcome is 8 turns are the most appropriate choice for the balance of tuning the frequency and obtaining the proper -38 dB value the outcome of efficiently working in terms of S11 parameters. In table 3.2, there is the comparison for the comparison of 6 and 7 turns.

Table 3.2 : Comparison of number of turns.

Center Frequency (GHz)	Diameter (mm)	Spacing between turns (mm)	Number of turns	Axial Length (mm)	Ws (Width of Strip, mm)	Return Loss (dB)
2.6	42.1	33.1	6	1.98.6	6	-13
2.7	42.1	33.1	7	231.3	6	-33

3.4 Comparison of Spacing between Turns

Although antenna works best at quarter-wavelength 0.22λ. With 0.25λ frequencies rises higher values to between 2600 – 2700 MHz but with 0.15λ spacing the frequency of antenna gets closer to center frequency 2400 Mhz. Also, the axial length of the antenna diminishes, which is a positive outcome with respect to the placement within the CubeSat. In table 3.3, there is the comparison for the comparison of spacing between turns between 22.2, 33.1 and 37.1 mm.

Table 3.3 : Comparison of spacing between turns.

Center Frequency (GHz)	Diameter (mm)	Spacing between turns (mm)	Number of turns	Axial Length (mm)	Ws (Width of Strip, mm)	Return Loss (dB)
2.65	42.1	22	7	176	5	-32
2.85	42.1	33.1	7	231.3	5	-26
2.5	42.1	37.1	7	259.1	5	-12

Table 3.4 : Center frequency tuning.

Center Frequency (GHz)	Diameter (mm)	Spacing between turns (mm)	Number of turns	Axial Length (mm)	Ws (Width of Strip, mm)	Return Loss (dB)
2.41	42.1	19.8	7	138.8	7	-33
2.32	42.1	33.1	7	198.6	5	-19
2.26	42.1	25	7	200	4	-20

In Table 3.4, some of the S11 values which are close to center frequency and RF performance are shown. The helix (Dh) is 42.1 mm calculated from the antenna theory formulas. The impedance matching strip is a piece of copper with the (Dh/4) 25 mm length, 6 mm width and 0.2 mm thickness. They show higher S11 values, meaning poorer matching and reduced efficiency. Similarly, increasing the electrical length (Ln = 954.1 mm) slightly shifts the resonance lower but does not necessarily improve return loss. The 6 mm substrate width (Ws) provides the best balance of impedance matching and bandwidth.

Overall, the balance of high number of turns optimized spacing between turns calculated diameter of helix provide sufficient level of radiation characteristics. In this graph it is visible each optimized with different structural parameters and searched for them most efficient helix geometry stable and efficient RF performance over a controlled frequency range 6 MHz bandwidth and strong impedance matching. The helical conductor wound around an axis with spacing of the range 20 and 33.1 millimeter between each turn.

The axial length of the antenna wire is the range of 130 mm – 240 mm, creates a right-hand circular polarization (RHCP). The number of turns defines the radiation characteristics such as gain, bandwidth and beamwidth. A higher number of turns increases the antenna gain but also affects impedance matching. The ground plane with a diameter same as the wavelength (132.3 mm). contributes as a reflector, provides directional characteristics by preventing the antenna radiate in opposite directions.

Future experimental validation through laboratory testing will help refine the design and ensure compatibility with mission requirements. At the operational frequency of 2.267 GHz the wavelength is 132.3 mm making the 22 mm spacing on the CubeSat suitable for the 1 wavelength criteria. The back to the front ratio proves the directivity is accomplished in figure 3.4. Calculated beamwidth is 45.08 by the equation (1.3) and the simulated beamwidth is as shown in Figure 3.4.

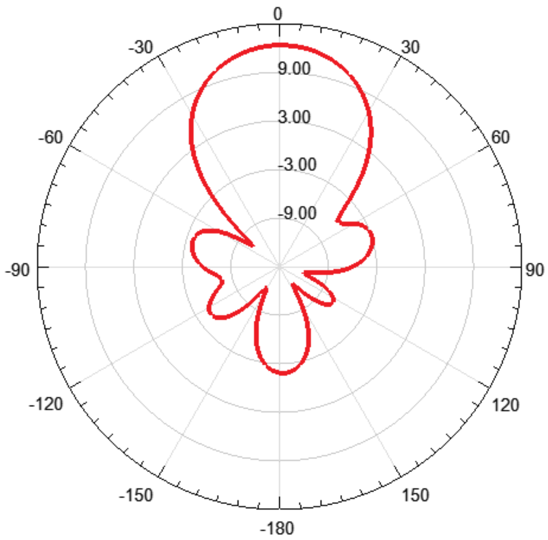

Figure 3.4 : Simulated gain plot of the antenna design.

Curve Info	xdb10Beamwidth(3)
dB(GainTotal) Setup3 : LastAdaptive Freq='2.267GHz' N='8' Phi='0deg' Ws='7mm'	45.8769

Figure 3.5 : Simulated beamwidth of the antenna.

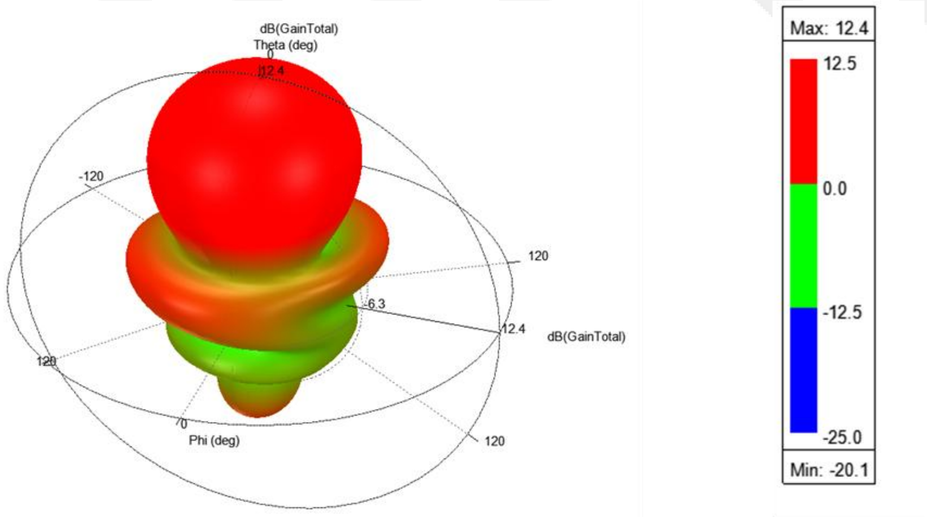

Figure 3.6 : Simulated radiation pattern of the antenna design.

The axial mode of configuration refers to main lob approaches along the helix axis, making communication ideal for satellite and the polarization is circular. Thus, the alignment with the ground station is another constraint and challenge. The simulated gain value is 12.4 dB as seen in Figure 3.6.

3.5 Feeding Mechanism

50-Ω feed line can be attained by keeping the antenna measurements fixed and centering the ratio of the inner diameter of the helix and conductor diameter. A Helix with $D \approx \lambda/\pi$ and $S \approx 0.22\lambda$ has an impedance of ~140 Ω, it needs matching for 50 Ω for system it can be e.g., λ/4 transformer is VNA tuning ±5% should be ended as tolerance adjustment based on actual measurements.

3.6 Feed structure and impedance matching

Coaxial feed mechanism which provides strong impedance matching and minimizes signal loss is assigned for signal excitation. The outer conductor wire has 4.3 mm diameter and the inner conductor also has 1.3 mm diameter which promises for a controlled impedance profile. The feed is placed 6 mm from the conductor during simulation, this allows for optimized coupling between the feed and the mechanism which is important for input impedance matching, effecting return loss and overall antenna efficiency. The feed transmission engages in the helical conductor easily ensuring smallest reflections and stable impedance matching to transmission line.

The conductor layer alters 0.5 mm thickness or first structural stability they do not have many impacts on radiation performance. The length of the coaxial feed which is 10 mm is defined to interact efficiently with RF subsystem while sustaining the compact form the antennas helical diameter and pitch angle are designed to optimize characteristic purity and directional radiation pattern which brings an axial mode for operation promises the main law is a line with the Helix axis provides ideal directional satellite communication on condition with alignment provided. There are so many techniques for placing a strip to the beginning of helix.

Impedance Matching formula,

$$Z = 140 \times \frac{C}{\lambda}(\Omega) = 140\Omega \tag{3.1}$$

The characteristic impedance Z of a helical antenna can be approximated by the formula, where C represents the circumference of the helix and λ is the operating wavelength. Typically, when the ratio $\frac{C}{\lambda}$ is close to one, the impedance is approximately 140 ohms. This impedance value is important for ensuring proper impedance matching between the antenna and the transmission line, which maximizes power transfer and minimizes signal reflection [13].

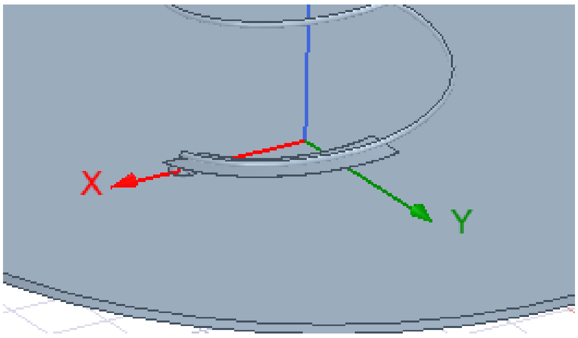

Figure 3.7 : Impedance matching strip.

Figure 3.8 : Manufactured strip soldered to SMA connector and conductor antenna wire.

The strip demonstrated in figure 3.7 and 3.8 additionally serves to improve impedance matching with its thickness of this strip altering the RF performance of the antenna. The optimized thickness of strip for input impedance matching part is 6 mm with the thickness of 35 µm. It optimized current distribution and minimized all make losses. The examination of strip dimensions is demonstrated in Table 3.5.

Table 3.5 : Comparison of width of strip.

Center Frequency (GHz)	Diameter (mm)	Spacing between turns (mm)	Number of turns	Axial Length (mm)	Ws (Width of Strip, mm)	Return Loss (dB)
2.34	42.1	22	7	176	4	-29
2.52	42.1	22	7	176	5	-46
2.3	42.1	22	7	176	6	-18

3.7 Material Selection

In space, environmental conditions are drastically different than the Earth which have critical consequences. The key environmental influences on the structure are radiation is sources by the Sun and deep space. Additionally, long launch vibration, friction between components can be considered as high-level risks.

Outgassing is one of the most crucial risks can be defined as the release of gases or what pores from solid materials when they are exposed to vacuum or high temperatures which can corrupt sensitive instruments like electronic boards, optics, cameras, lenses, solar panels which can cause the reduction of their performance hence it can lead heat dissipations which complicates thermal control.

Structurally, materials become more brittle when they are exposed to outgassing some certain materials like silicone, rubbers, polyamide and resins they cause high outgassing and does not show proper behavior for space applications therefore materials for space structures are picked according to space qualified materials like carbon fibers, PTFE, PEEK, aluminum and processed copper as shown in Figure 3.9 and 3.10. The consideration is relevant for antennas because they must maintain long term reliability and performance in orbit.

To reduce the negative influence of outgassing engineers develop techniques like prebaking components in vacuum chamber or to anodize these materials to seal surfaces with coating like perylene. Organizations like NASA and ESA encourage companies to ensure material compatibility and safety during missions [38].

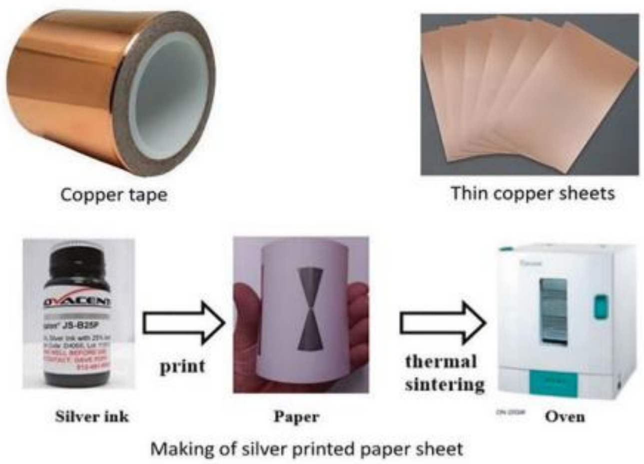

Figure 3.9 : Conductive materials for fabricating origami antennas.

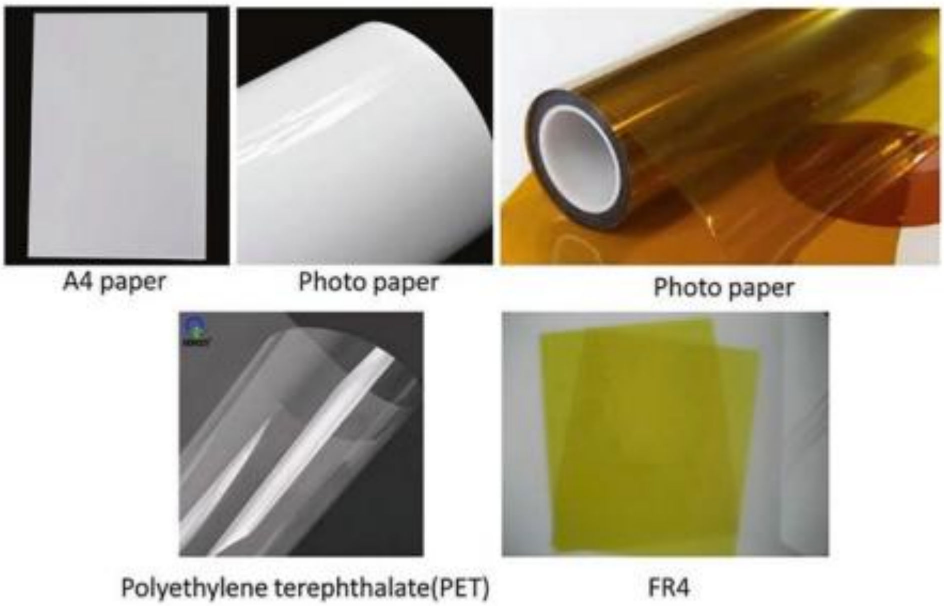

Figure 3.10 : Dielectric materials for fabricating origami antennas [44].

Another aspect in material selection is considering materials according to RF performance. High accuracy for thermal ranges and reflect ability is crucial factors must be addressed. A deployable satellite antenna necessarily operates between the temperature limits of 110 °C down to -70 °C [26]. Material should be stiff and high strength to preserve with minimum distortions. Zero gravity refers to almost no loads after launch. Before settling into the orbit, it should be guaranteed the materials will withstand during launch electromagnetic and mechanical properties should maintain for post-launch. Therefore, plastic films like mayor and polyamide also can be manufactured as vacuum metalized which are a thin layer of aluminum on the surface which provides high reflective features and low surface resistance [34].

Polyamide, the scientific brand name is Kapton® 300 HN polyimide film, with lightweight, good electromagnetic performance and flexibility of metallized films which makes the material excellent option for space antennas. Material properties are listed in Table 3.6.

Table 3.6 : Material properties comparison.

Material	Linear CTE (µm/m°C)	Resistivity (Ohm-cm)	Density (g/cc)	Yield Tensile Strength (MPa)	Modulus of Elasticity (GPa)
Aluminum 7076-T61	21.6	4.30E-06	2.84	470	67
Beryllium	14.5	4.30E-06	1.844	240	303
BeNi M220C	14	2.87E-05	8.03	1100	180
Nitinol (Low Temp)	NA	7.60E-05	6.45	100	28
Nitinol (High Temp)	NA	8.20E-05	6.45	560	70
HexPly M47 Carbon Prepreg	NA	NA	NA	920	40
285 Kevlar Prepreg	NA	NA	NA	558	20.7
7791 E-Glass Prepreg	NA	NA	1.39	372	NA
48 Gauge Mylar	17.0	NA	1.39	179	NA
Kapton HN	20.0	NA	1.42	70	NA

Table 3.7 : Comparison table for different origami antennas [31].

Substrate Material	Antenna Type	Frequency (GHz)	Gain (dB)	Polarization
Paper	Yagi-Uda	0.69-0.80	4-8	Linear
Paper	Helical	1.28-4.12	6, 8.5, 5	Linear, RCHP Elliptical
Paper	Helical	0.86-3	-	Linear
Paper	Dipole	0.75-1.29	-0.48-3	Linear
Paper	Conical Spiral	1.4-3.7	7-12	Linear and circular
Paper	Helical	0.86-2.14	9.6	Linear
Multiple Papers	Monopole	2-4	5.2-5.7	Linear
Multiple Papers	Monopole	2.4-5	6.5-8	Linear
Multiple Papers	Yagi	0.65-1.8	6.5-8	Circular
Paper	Helical	0.650-1.8	10.4	Linear
Paper	Yagi	1.31	-	Linear
Paper	Helical	1.8-2560	9.7-14.7	Linear
Sketching Paper	Helical	2.07-4.45	10	LHCP
PET sheets	Yagi	1.7-2.8	-	Linear
PET sheets	Yagi	2.2	-	Linear
FR4	Patch	2.45	3, 8	Linear
FR4	Array	2.4	1-12	Linear
FR4	MIMO	2.33-2.91		Linear
PTFE	Patch	1.98-2.2	12.6	Circular
Photo paper	Monopole	2.3-7	3.7-4.9	Linear

In Table 3.7, the variety of electrical performance, durability, flexibility, and adaptation with space environment are core elements to consider while choosing material and designing a helical antenna for space. The Antenna consists of different elements such as helical conductor and ground plane. Also, it is seen in the table that the helical antennas which are in normal mode have linear polarization. To have circular polarization helical antennas should be in axial mode.

For helical conductor candidates are copper, silver, gold, and aluminum which are detailed examined. Highly conductive wire to diminish the loss and sustain efficient radiation. Copper in RF applications is very conductive (5.8×10^7 S/m) to avoid oxidation gold coating play pink can be utilized. Silver plating is considered as a promising option since the silver (Ag) has the highest conductivity (6.3×10^7 S/m) metals. Although gold (Au) plating is commonly used in most space applications, it was deemed too expensive for this project. Therefore, silver coating over copper was used as a more cost-effective alternative [26].

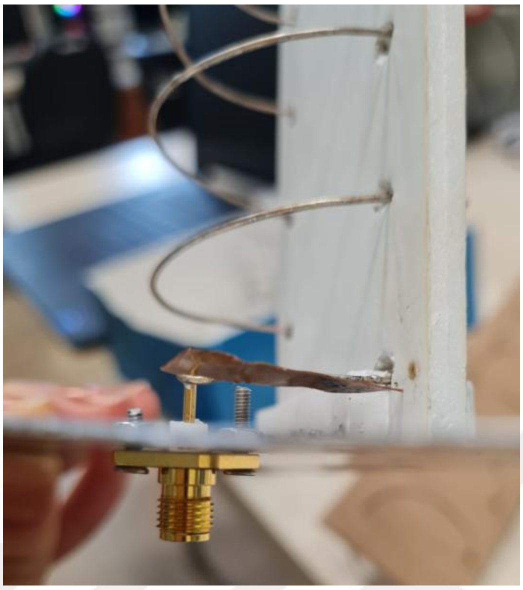

Figure 3.11 : SMA connector with ground plane.

- For the ground plane, the priority is good reflectivity to electromagnetic waves for material selection. Cooper, carbon fiber is your options are your immune strength lightweight and Ground Plane: The ground plane should be constructed from a material that provides good reflectivity to electromagnetic waves. Al 6061-t6 or 7071 offers light weight and it is common for space proposes usage. Its conductivity (3.7×10^7 S/m) Aluminum anodized copper to increase endurance anodization technique can be used.
- Coaxial Feed Structure: A SMA connector shown in the figure 3.10 is used as a coaxial feed which has a pin in the center as a conductor and a shield as an outer conductor divided by a dielectric layer behaving like a coaxial cable. This enables efficient transmission signals with minimal losses and thermal stability. It has typically 50 Ohm impedance. They are used as wireless communication devices, test equipment and antenna connections.

Future experimental validation through laboratory testing will help refine the design and ensure compatibility with mission requirements. With the corresponding to the central 2267 MHz frequency the wavelength of 132.3 mm and the design is optimized around this value.

4. FABRICATION

Trials with various materials such as paper, Teflon (PTFE), and polyamide were conducted to evaluate different types of origami. Kapton, a type of polyamide, was chosen due to its flexibility and ease of folding. While prototyping with PTFE material, the technique is to diminish stress by cutting out holes at joint edge points and to create spots to have antenna wire to pass through and find a proper path the wire can follow is tested. It was observed that the material, being notably stiffer than paper, reacted to the forces applied through the holes by creating extra tension. As a result, the use of holes at hinge points was abandoned.

The dimensions for the RF components were guided by simulations in HFSS and validated through testing with a spectrum analyzer. For example, aluminum plate with a diameter of 10 cm was used as the ground plane is cut by press machine.

Figure 4.1 : Mockups during process.

During the development process, it is considered several deployment mechanisms, including rollable, truss, and telescopic booms made from different materials. Some of the mockups are shown in Figure 4.1 executed with paper, polyamide and Teflon. The polyamide sheet was cut using a laser machine. To find the correct folding configuration, it is designed mockups with one-piece, two-piece as seen in Figure 4.4, and three-piece configuration and two-piece configuration were applicable. However, repeated laser passes at the same location caused damage to the sheet. To mitigate this condition, two methods are combined which are laser cutting for precision and manual scoring for partial cuts.

However, it has the disadvantage of tending to tear easily. If there is a small crack under force, therefore execution must be completed without harm. In case of deformation, the material behaves like glass. Cracks tend to propagate toward the edges of the structure. The stiffness and solidity of the polyamide material balance its this feature. The goal was to create a folding pattern without causing any material failure. Finally, after multiple sessions of laser cutting and 3D printing, the final model was assembled using screws and bolts, as shown in Figures 4.2 and 4.3.

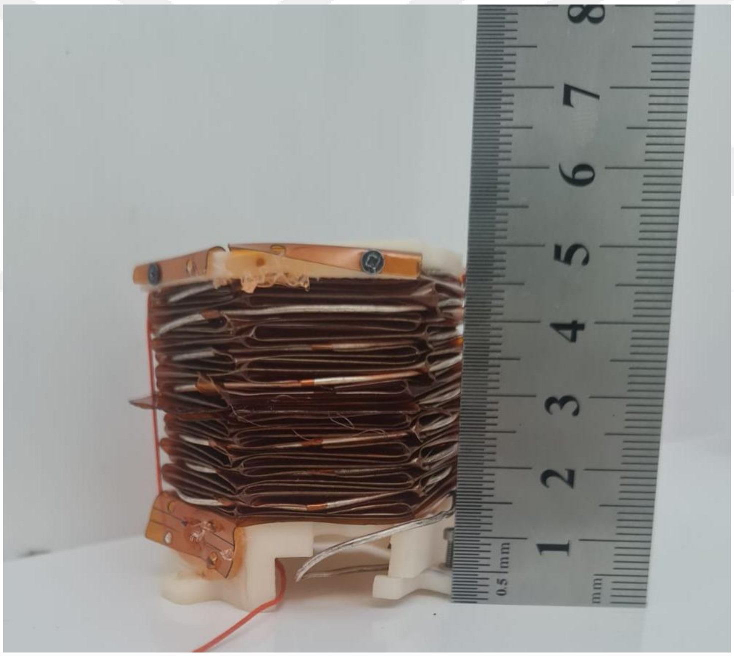

Figure 4.2 : Stowed version of antenna (45 mm).

Figure 4.3 : Deployed version of antenna (176 mm).

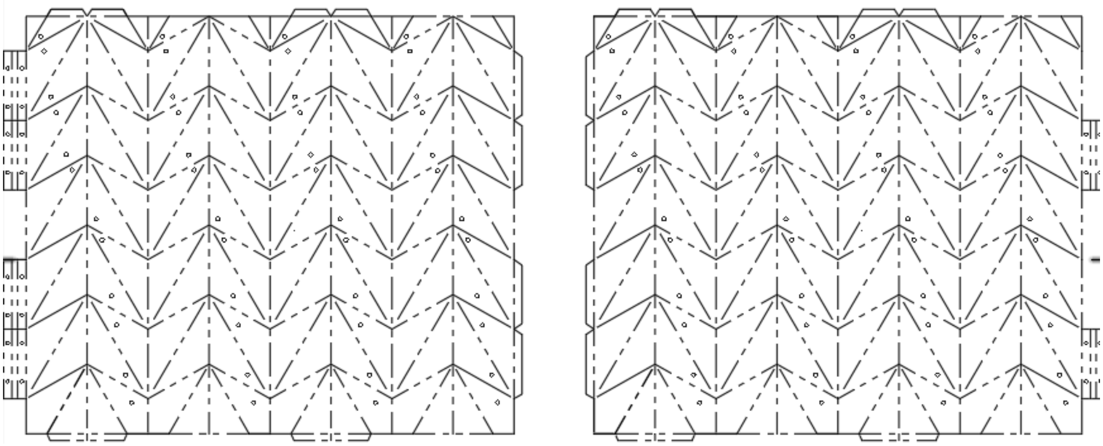

Figure 4.4 : 2D drawing of the polyamide sheet.

4.1 The Goal of the Structure

The purpose of the structure is to create a deployable system that maintains the helical antenna in a vertical and stable direction, pointing toward the ground station. Since this is a directional antenna, it is essential to ensure consistent structural features which must therefore be reliably stable throughout the deployment, launch and operation phases. The main approach behind the design is the mutual relationship between the polyamide Kapton sheet and conductive silver coated cooper wire in terms of solidity and stiffness.

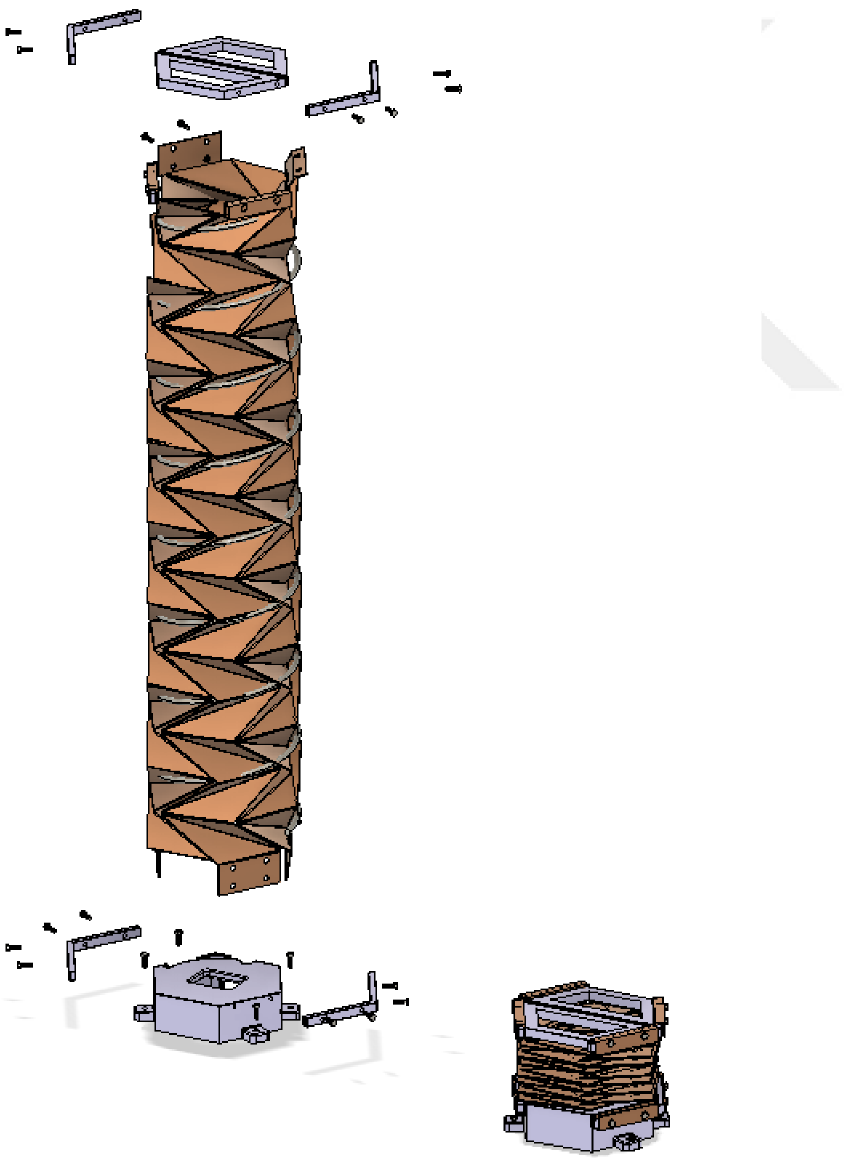

Figure 4.5 : Exploded CAD model of antenna.

4.1.1 Actuators for deployable antennas

Deployment mechanisms can be divided into two main categories which are strain energy-based deployers and motorized deployers (Sullivan, 2020). These two divisions can be branched out into various types of actuation systems, for instance soft pneumatic actuators, shape memory alloy actuators, shape memory polymer actuators and 4D-printed self-actuators. The locking and releasing system is designed with an emphasis on using lightweight components, as minimizing mass is a key consideration throughout the design process [30].

4.1.2 Locking releasing security mechanism

The mechanism consists of redundant resistors and melting springs. The resistor circuit is placed on the main board. For deployment hold and release system works fit bottom and upper place plate in between these platforms.

As it is demonstrated in the figure 4.8 and 4.9, the origami structure is placed and specialized dyneema wire made in Japan in the figure 4.10 is holding them together and with the help of the resistor the deployment happens.

Figure 4.6 : Employed dyneema wire.

Additionally, there are compression supports which combine the polyamide structure with the manufactured 3D prints, shown in the figure 4.7 and 4.8. Originally it is planned to manufacture the parts with aluminum 6061 but for prototyping 3D printing with FDM method and PLA material is used for the structural support parts which are shown in Figure 4.7 and for the manufacturer of origami structure laser cutting machine is used. The antenna assembly is secured using screws, along with extensions of the polyamide sheet and plates. Epoxy and 1.6M screws are used to hold the Kapton polyamide sheet and the supporting structure together, utilizing compression for added stability.

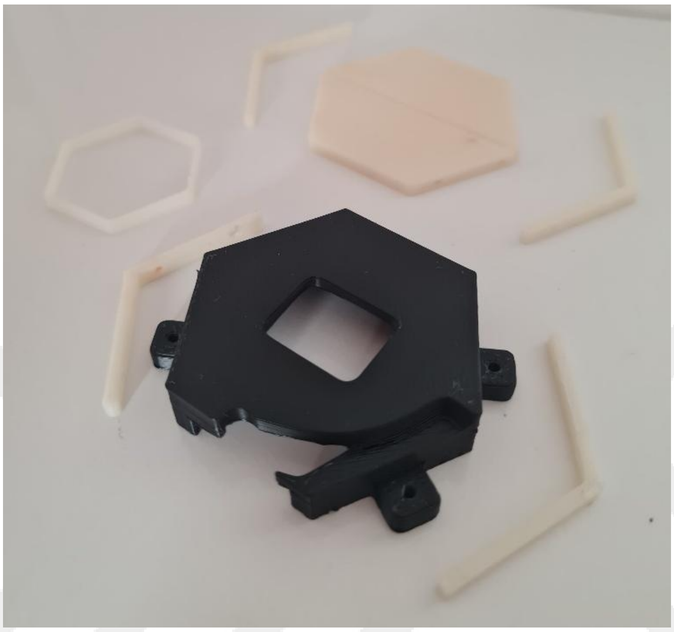

Figure 4.7 : 3D printed structure parts.

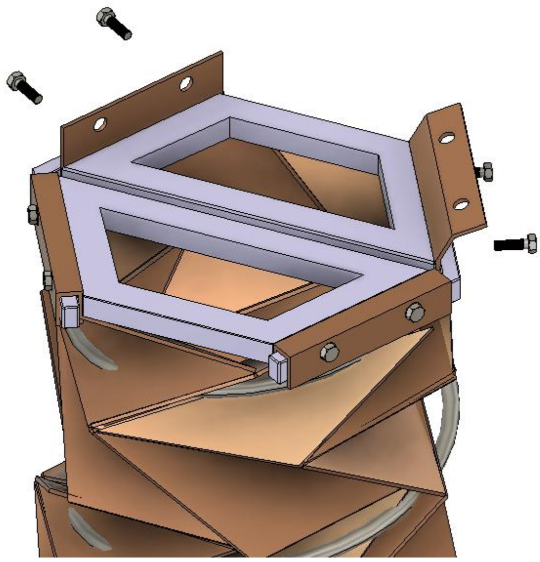

Figure 4.8 : Cross-section of the stowed elbowed boom.

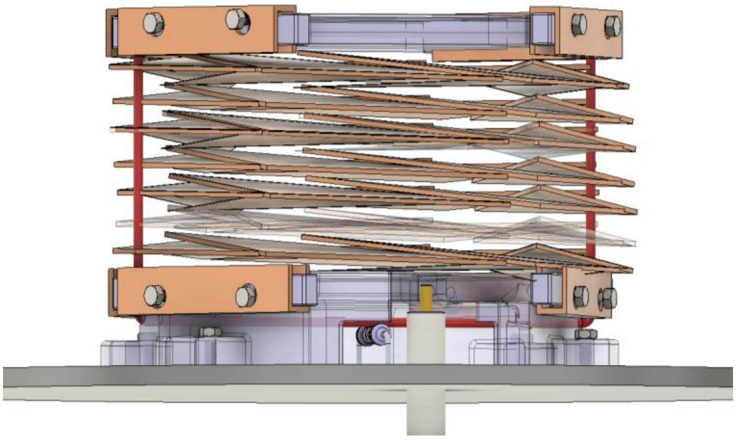

Figure 4.9 : Hold and release mechanism of the helical antenna.

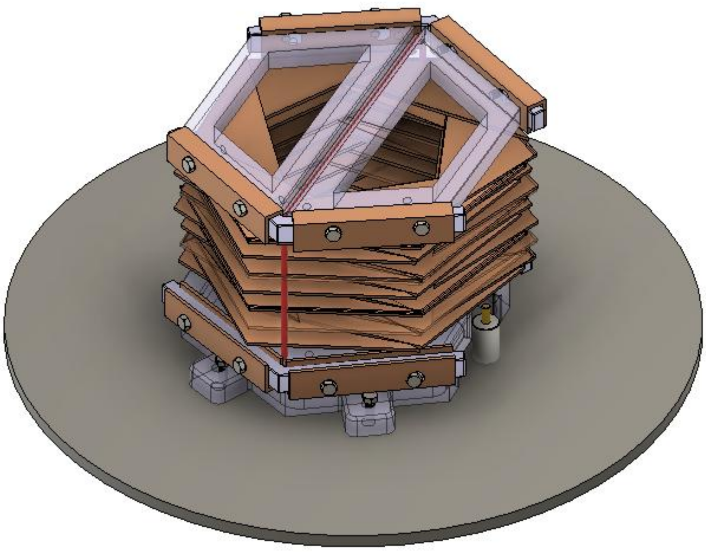

Figure 4.10 : Relationship between the antenna structure and dyneema wire.

Figure 4.11 : Storage Stability Test Model.

Some tests on the Dyneema wire were conducted over the course of one month. During this period, the system was kept in the stowed position, tied using a Surgeon's knot. No loosening was observed in the stowed configuration of the helical antenna throughout the test duration. Figure 4.11 shows the antenna in its stowed state after one month. It was a storage stability test considering the spacecraft might wait for a period of time in space facilities before they are launched and deployed into space by simulating the possibility of this scenario.

4.2 Structure Design and Placement Requirements

As shown in Figure 4.11, ISIS Space presented the standards of the CubeSat dimensions with a technical drawing. Cylindrical volume called tuna can, measuring 40 (height) × 80 mm (diameter) is included volume constraints. Since the dimensions of the stowed version of the design is 35 × 60 mm, it does not exceed the limits of the standard. The design ensures necessary accommodation within the tuna can boundary defined for CubeSat structures. This is an important consideration of structural antenna design.

Not only the main CubeSat structure but the stowed payloads such as antennas, solar panels and sensors must stay within defined limits. This requirement is related to the deployment pod, as the CubeSat must fit inside to be integrated into the launcher rocket.

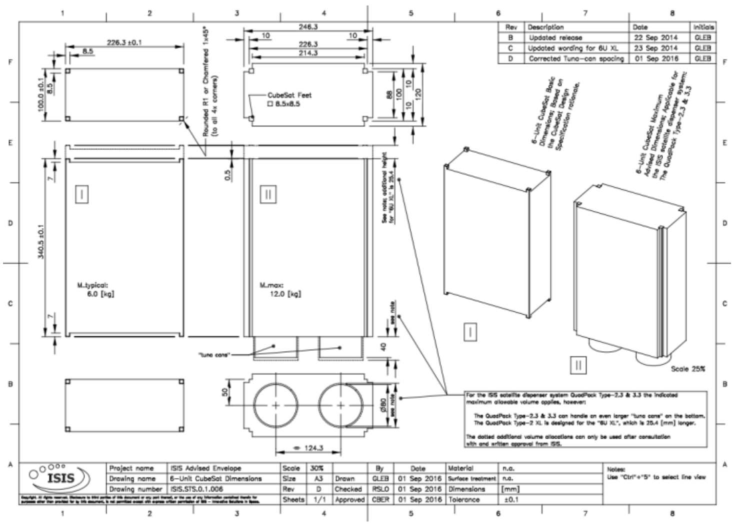

Figure 4.12 : 6U CubeSat Dimension [41].

Figure 4.13 : Rendering of deplored version of helical origami antenna with 6U CubeSat configuration.

5. SIMULATIONS AND TESTS

5.1 S11 Measurements

The test setup antenna which is seen in Figure 5.2 is 60 gr. During S11 testing consists of two phases and the impedance matching process with copper strip was a trial-and-error approach until the antenna shows resonant behavior. It is a method to understand how to solder the matching patch to antenna according to reaction of the antenna cutting them or adding them together. At first during test, it is obtained – 38 dB min value and additionally with zig zag pattern in the graph which proves that the impedance matching can be developed. In the second test, there was visible a defined bandwidth with dependable curve.

Figure 5.1 : S11 spectrum results.

The result shown in Figure 5.1 promises good impedance matching and the good entrance of signal to the antenna which means the antenna is ready for communication testing and anechoic chamber testing and shows the behavior of the antenna in wideband with 0 dBm output power. The span was in between 1.3 – 3.3 GHz. Center frequency was centered in the span which is 2267 MHz..

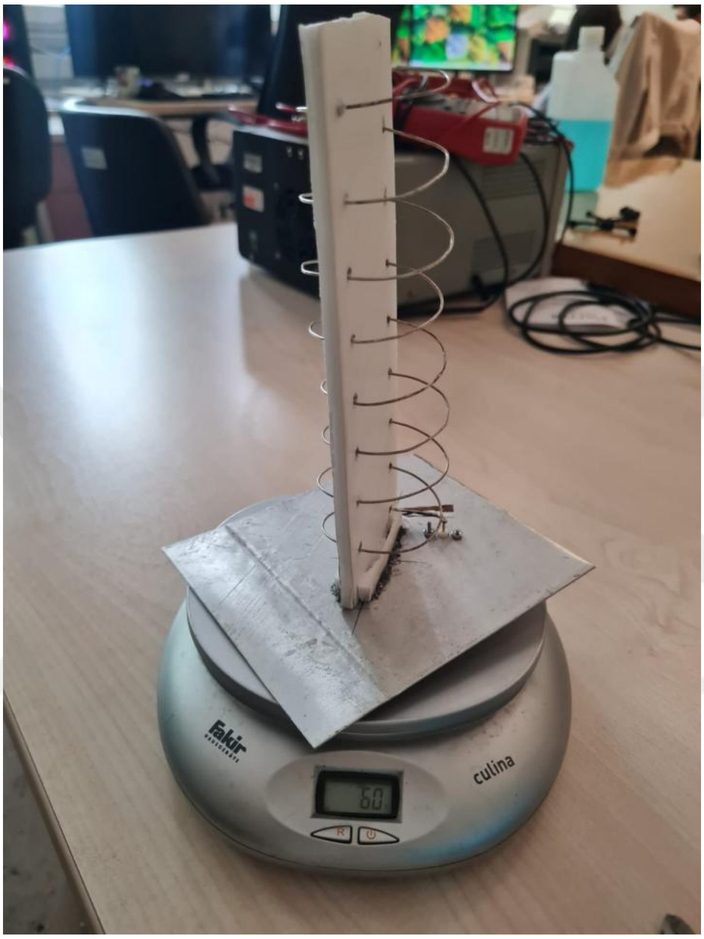

Figure 5.2 : The test setup antenna.

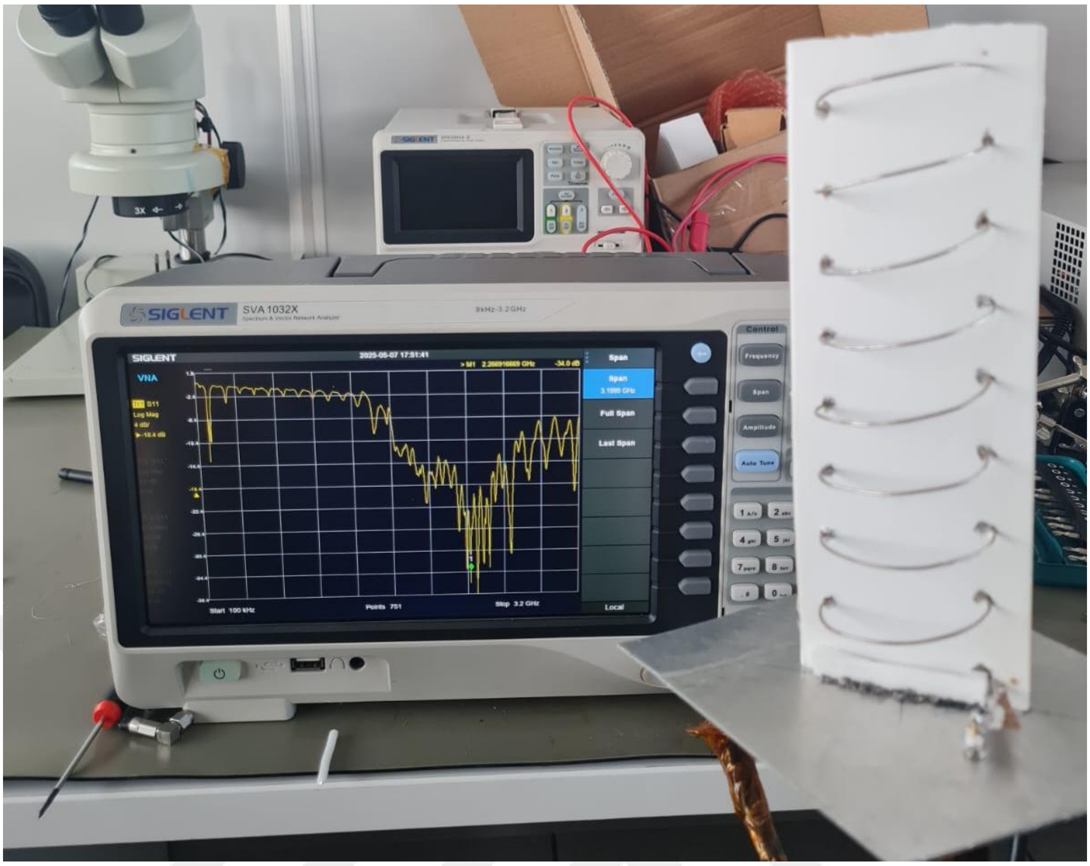

Figure 5.3 : Initial S11 spectrum testing of the antenna.

In figure 5.3, it is seen S11 values which have sharper zig zag pattern it demonstrates antenna with low impedance matching which interrupts the wide bandwidth even though center frequency is powerful. With impedance matching the curve became more fluent as it is seen earlier in the section. Bandwidth is defined as 500MHz.

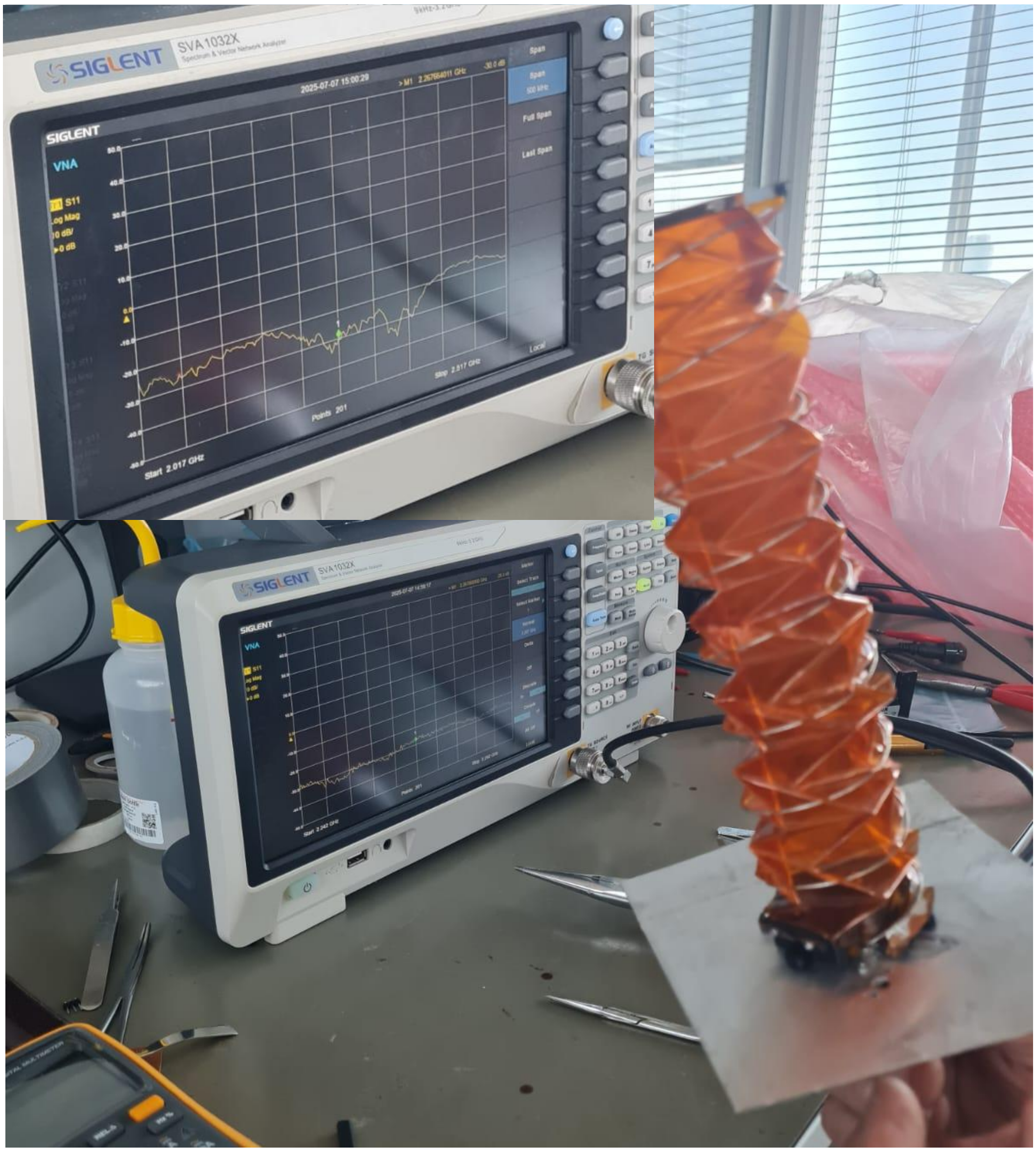

Figure 5.4 : Spectrum testing with origami structured helical antenna.

As seen in Figure 5.4, spectrum tests with origami structured antenna also conducted and -30 dB return loss achieved which proves the antenna operates in defined frequency with wide bandwidth with impedance matching. The rendering of antenna and CubeSat configuration is demonstrated in Figure 5.5.

5.2 Anechoic Chamber Tests

Anechoic chambers (see Figure 5.5) annihilate the environmental effects of electromagnetic waves, sound or any kind of object and vibrations to prevent the degradation and reduction of RF performance which the basics are schematized in

Figure 5.6 which is in this case it is a hybrid system. Different materials are used to balance the operating frequency bands and involve low frequencies bands [50].

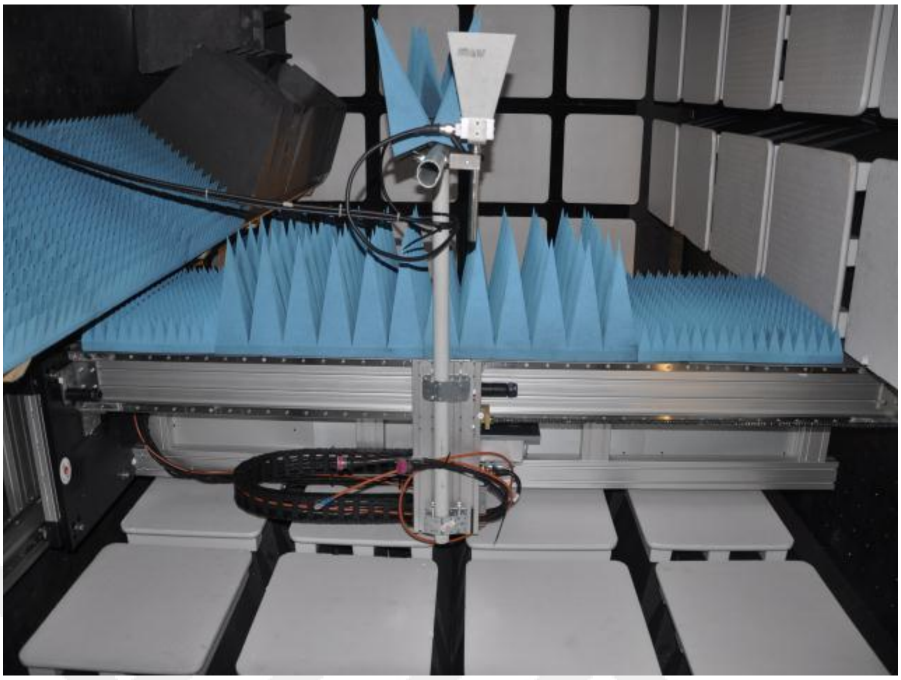

Figure 5.5 : Anechoic chamber test environment.

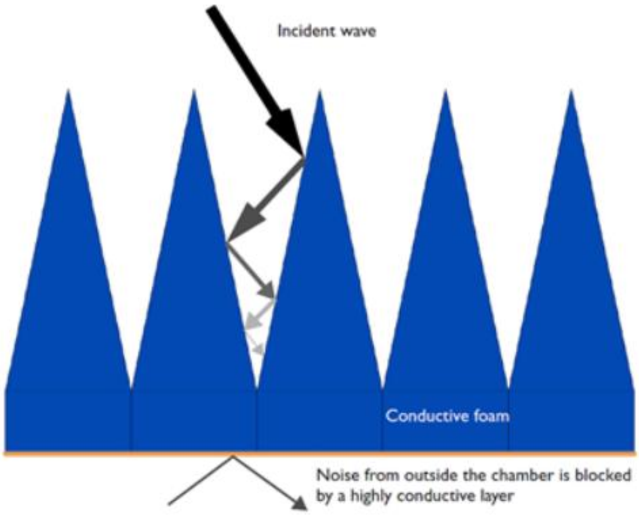

Figure 5.6 : Pyramidal RAM absorbs the incident signal.

The network analyzer was calibrated to eliminate the influence of cable and connectors as seen in the Figure 5.7 and provided S_{11} (return loss or antenna matching), S_{12} (the amount of the power transmission from Port 1 to 2), S_{21} (from Port 2 to 1), and S_{22} (the amount of the power reflected back from Port 2) measurements.

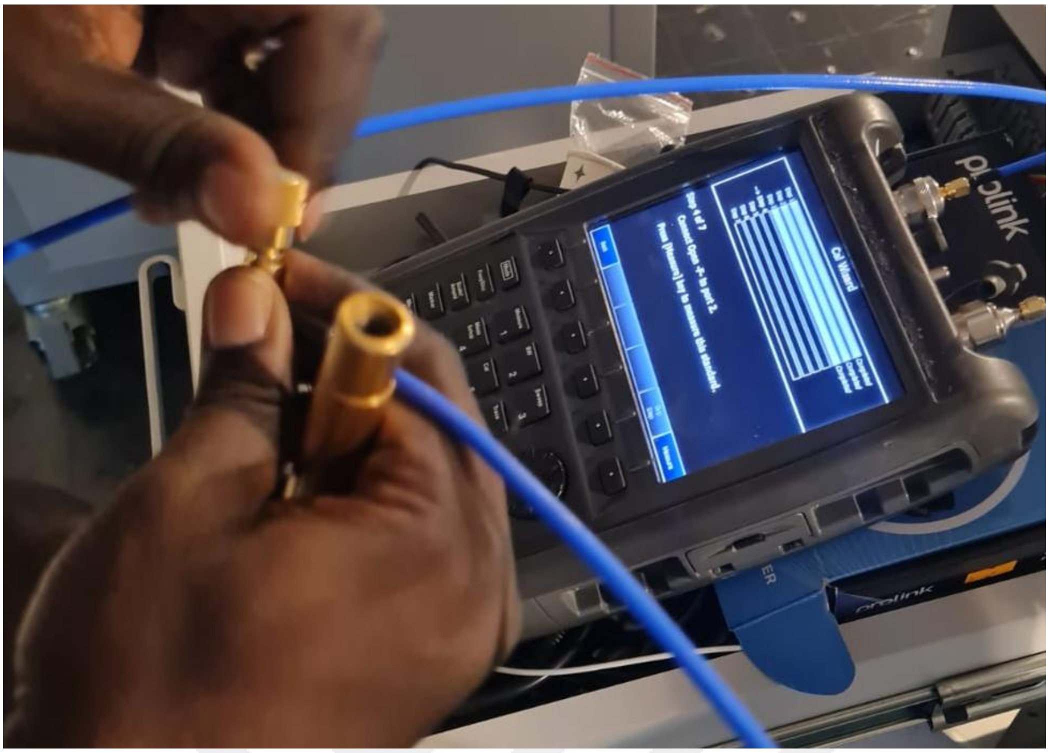

Figure 5.7 : Calibration of the spectrum analyzer.

The output power was –15 dBm, and the bandwidth was 10 kHz, as shown in Figure 5.9. During the test, the distance between the antennas was 2 m, and the antenna height was 125 cm. The gain of the employed horn antenna near the center frequency (2.2 GHz) is 9.5 dBi.

For the test, the helical antenna and a horn antenna were placed facing each other as two portsas shown in the Figure 5.8. Port 1 is a helical antenna and port 2 is a horn antenna. $S_{12}$and S_{21}values remained consistent across several angles. S_{11} parameter demonstrates the deep notch around −25 dB indicates good impedance matching at 2267 MHz.

Measurements were taken at various angles, including 10°, 45°, and 90°, confirming stable transmission and reception characteristics across different orientations. When the horn antenna was rotated between vertical and horizontal directions, no significant change was observed in the measured values which is a desirable outcome ensuring polarization stability. Since the test setup was not automated, the gain of the origami structured antenna calculations will be conducted after analyzing the result of each angle.

Figure 5.8 : The test setup with origami structured helical antenna.

Figure 5.9 : Network analyzer test results.

The S_{11} and S_{22} values indicate good impedance matching at both ports, and the S_{21} and S_{12} values show efficient power transfer and isolation between ports in both forward and reverse directions.

6. CONCLUSION AND FUTURE WORK

With this project, it is aimed to suggest an innovative and feasible design for deployment mechanisms of CubeSat antennas. It can be also considered for other kinds of deployment mechanisms other than only antennas such as space habitat concepts as a futuristic approach. As the future work system can be designed safer for launch process considering such forces as g-forces and vibration. For deployment detection microswitch can be considered to evaluate whether the antenna is deployed or not and it can be tested with other kinds of conductive materials.

REFERENCES

[1] **Kulu E. (2019).** “Nanosats Database,” *https://www.nanosats.eu/, accessed 2019 10-06.*

[2] **Olson, G., Pellegrino, S., Costantine, J., & Banik, J. (2012, April).** *Structural architectures for a deployable wideband UHF antenna. In 53rd AIAA/ASME/ASCE/AHS/ASC Structures, Structural Dynamics and Materials Conference 20th AIAA/ASME/AHS Adaptive Structures Conference 14th AIAA (p. 1836).*

[3] **RC Model Reviews. (2012, May 14).** *How do antennas work? (August 30, 2017) [Video]. YouTube. https://www.youtube.com/watch?v=fSoXIqBlg9M.*

[4] **Liu, S., Theoharis, P. I., Raad, R., Tubbal, F., Theoharis, A., Iranmanesh, S., Abulgasem, S., Khan, M. U. A., & Matekovits, L.** (2022). A survey on CubeSat missions and their antenna designs. Electronics, 11(13), 2021. https://doi.org/10.3390/electronics11132021.

[5] **Yao, S., Georgakopoulos, S., Cook, B., & Tentzeris, M.** (2014). A novel reconfigurable origami accordion antenna. Proceedings of the IEEE MTT-S International Microwave Symposium (IMS), Tampa Bay, FL, USA. https://doi.org/10.1109/MWSYM.2014.6848571.

[6] **Yao, Shun.** (2017). "Origami Reconfigurable Electromagnetic Systems" FIU Electronic Theses and Dissertations. 3514. https://digitalcommons.fiu.edu/etd/3514.

[7] **ESA eoPortal. (n.d.).** (2025). GOMX-3 (GomSpace Express-3). eoPortal Directory. from https://www.eoportal.org/satellite-missions/gomx-3.

[8] **Costantine, J., Tawk, Y., Maqueda, I., Sakovsky, M., Olson, G., Pellegrino, S., & Christodoulou, C. G.** (2016). UHF deployable helical antennas for CubeSats. IEEE Transactions on Antennas and Propagation, 64(9), 3752-3759.

[9] **Dolapçı, T.** (2020). Design, simulation, and fabrication of CubeSat antenna systems (Master’s thesis, Middle East Technical University). Graduate School of Natural and Applied Sciences, Middle East Technical University.

[10] **Tariq, S., & Baktur, R.** (2015). Circularly polarized UHF up-and downlink antennas integrated with CubeSat solar panels. In 2015 IEEE International Symposium on Antennas and Propagation & USNC/URSI National Radio Science Meeting (pp. 1424-1425).

[11] **Slade, B.** (2015). The basics of quadrifilar helix antennas. Orban Microwave Inc., Orlando, FL, USA.

[12] **Abulgasem, S., Tubbal, F., Raad, R., Theoharis, P. I., Lu, S., & Iranmanesh, S.** (2021). Antenna designs for CubeSats: A review. IEEE Access, 9, 45289-45324.

[13] **Huang, Y., & Boyle, K.** (2008). *Antennas: From theory to practice*. John Wiley & Sons.

[14] **Cisco Systems, Inc.** (2007). Antenna patterns and their meaning. Cisco Systems, Inc. ESA eoPortal. (n.d.). *GOMX-3 (GomSpace Express-3)*. eoPortal Directory. Retrieved June 11, 2025, from https://www.eoportal.org/satellite-missions/gomx-3.

[15] **Kraus, J. D., & Marhefka, R. J.** (2002). Antenna theory: Analysis and design (3rd ed.). McGraw-Hill.

[16] **Shami A. and Maier M.** (2010). "Link adaptation," in *Broadband Access Networks: Technologies and Deployments*, Springer.

[17] **Balanis, C. A. (2015).** Antenna theory: analysis and design. John wiley & sons.

[18] **Muri, P., Challa, O., & McNair, J.** (2010). Enhancing small satellite communication through effective antenna system design. In 2010-MILCOM 2010 MILITARY COMMUNICATIONS CONFERENCE (pp. 347-352).

[19] **Olson, G., Pellegrino, S., Costantine, J., & Banik, J.** (2012). Structural architectures for a deployable wideband UHF antenna. In 53rd AIAA/ASME/ASCE/AHS/ASC Structures, Structural Dynamics and Materials Conference 20th AIAA/ASME/AHS Adaptive Structures Conference 14th AIAA (p. 1836).

[20] **Fei, F., Leng, Y., Xian, S., Dong, W., Yin, K., Zhang, G.** (2022) Design of an Origami Crawling Robot with Reconfigurable Sliding Feet. Appl. Sci., 12, 2520. https://doi.org/ 10.3390/app12052520.

[21] **Charles, R. A.** (2000). *Design, construction and testing of the deployable UHF antenna for Skynet 4 Stage 2*. In S. Pellegrino & S. D. Guest (Eds.), *IUTAM-IASS Symposium on Deployable Structures: Theory and Applications* (pp. 77–86). Springer. https://doi.org/10.1007/978-94-015-9514-8_9.

[22] **Kobza, C. R.** (2016). *Space qualification testing of a shape memory alloy deployable CubeSat antenna* (Master's thesis, Air Force Institute of Technology). Air University. https://apps.dtic.mil/sti/pdfs/AD1018256.pdf.

[23] **Tibert, G.** (2002). Deployable tensegrity structures for space applications (Doctoral thesis, Royal Institute of Technology). KTH. https://www.researchgate.net/publication/244457217.

[24] **Sureda M.** (2021). "Design and Testing of a Helix Antenna Deployment System for a 1U CubeSat," in IEEE Access, vol. 9, pp. 66103-66114, doi: 10.1109/ACCESS.2021.3075660.

[25] **Patnam, R. H.** (2008). Broadband CPW-Fed Planar Koch Fractal Loop Antenna. *IEEE Antennas and Wireless Propagation Letters, 7*, 429-431.

[26] **Auslander, D., Cermenska, J., Dalton, G., de la Pena, M., Dharan, C. K. H., Donokowski, W., Duck, R., Kim, J., Pankow, D., Plauche, A., Rahmani, M., Sulack, S., Tan, T. F., Turin, P., & Williams, T.** (2008). *Instrument boom mechanisms on the THEMIS satellites: Magnetometer, radial wire, and axial booms*. *Space Science Reviews*, *141*(1–4), 233–275. https://doi.org/10.1007/s11214-008-9386-4

[27] **Rezaei A. and Sumantyo D. S.** (2020). "Design and thermal analysis of a deployable satellite antenna for CubeSat applications." *IntechOpen*, [Online]. Available: https://www.intechopen.com/chapters/73013.

[28] **Belvin, W. K., Straubel, M., Wilkie, W. K., Zander, M. E., Fernandez, J. M., & Hillebrandt, M. F.** (2016). Advanced Deployable Structural Systems for Small Satellites.

[29] **European Space Agency.** (2024). *LacunaSat-2B successfully completes mission and deorbits sustainably*. European Space Agency. https://www.esa.int/Applications/Connectivity_and_Secure_Communications/LacunaSat-2B_successfully_completes_mission_and_deorbits_sustainably

[30] **Damkjar, S., Cupido, C., Nokes, C., Mann, I. R., & Elliott, D. G.** (2019). Design and Verification of a Robust Release Mechanism for CubeSat Deployables. *2019 IEEE Canadian Conference of Electrical and Computer Engineering (CCECE)*.

[31] **Shah, S. I. H., Bashir, S., Ashfaq, M., Altaf, A., & Rmili, H.** (2017). Lightweight and Low-cost Deployable Origami Antennas- A Review. *IEEE Access*.

[32] **ESA eoPortal. (n.d.). CubeRRT (CubeSat Radiometer Radio Frequency Interference Technology Validation). eoPortal Directory.** (2025). from https://www.eoportal.org/satellite-missions/cuberrt#rdb-radiometer-digital-backend

[33] **Bolton, S., Doty, D., & Rivera, P.** (2015). Compact Deployable Antenna for CubeSat Units. California Polytechnic State University, San Luis Obispo.

[34] **Onal C.D., Wood R.J., and Rus D.** (2011). "Towardsprintablerobotics: Origami inspired planar fabrication of three-dimensional mechanisms," in Proc. IEEE Int. Conf. Robot. Autom., Shanghai, China. pp. 4608 4613.

[35] **Huang T., Reveles J. R., Gurusamy V., Harrington Q., and Fraux V.** (2019**).** An innovative deployable VHF/UHF helical antenna for nanosatellites, in *Proc. 13th European Conference on Antennas and Propagation (EuCAP)*, Kraków, Poland, pp. 1–4.

[36] **Kresling, B.** (2008). Natural Twist Buckling in Shells: From the Hawkmoth's Bellows to the Deployable Kresling-Pattern and Cylindrical Miuraori. In J. F. Abel.

[37] **Cooke R. (Eds.)** (2008). Proceedings of the 6th International Conference on Computation of Shell and Spatial Structures, IASS-IACM.

[38] **National Academies of Sciences and Medicine.** (2015). Handbook of Frequency Allocations and Spectrum Protection for Scientific Uses; National Academies Press: Washington, DC, USA.

[39] **Molaei, A., Liu, C., Felton, S. M., & Martinez-Lorenzo, J.** (2018). Origami Inspired Reconfigurable Antenna for Wireless Communication Systems. *arXiv preprint arXiv:1805.10370*. https://arxiv.org/abs/1805.10370.

[40] **DuPont. (**2024). *Kapton® HN Polyimide Film: Product Data Sheet*, Doc. No. EI-10206. [Online]. Available: https://www.kapton.com

[41] **Innovative Solutions in Space B.V.** (2015) "6U CubeSat dimensions – ISIS.STS.0.1.006 Rev D Sheet 1-1," Dec. [Online]. Available: https://www.isispace.nl/wp-content/uploads/2015/12/ISIS.STS_.0.1.006-RevD-Sheet1-1-6U-CubeSat-Dimensions-A0.pdf.

[42] **Costantine J., Tawk Y., Ernest A. and Christodoulou C. G.** (2012). "Deployable Antennas for CubeSat and Space Communications," in *6th European Conference on Antennas and Propagation (EUCAP)*, pp. 837-840.

[43] **Knott, G., Viquerat, A., & Bojovschi, A.** (2018). Design of Deployable Helical Antennas for Space-Based Automatic Identification System Reception. Proceedings of Emerging Sensing Technologies Summit 2018.

[44] **Shah S. I. H., Bashir S., and Koziel S.** (2021). *Origami Antennas for Wireless Communication Systems*. Springer, doi: 10.1007/978-3-030-72187-6.

[45] **Chahat N., Hodges R. E., Sauder J., Thomson M., Peral E. and Rahmat-Samii Y.** (2016) "CubeSat deployable Ka-band mesh reflector antenna development for Earth science missions," *IEEE Transactions on Antennas and Propagation*, vol. 64, no. 6, pp. 2083–2091, doi: 10.1109/TAP.2016.2546306.

[46] **Aherne M. R., Barrett J. T., Hoag L., E. Teegarden, and Ramadass R.** (2012) "Aeneas -- Colony I meets three-axis pointing," *Space Engineering Research Center*, Marina del Rey, CA.

[47] **National Aeronautics and Space Administration. (n.d.).** *Origami Starshade*. Science.nasa.gov. Retrieved from https://science.nasa.gov/resource/origami-starshade/

[48] **Yao, S.** (2017). "Origami Reconfigurable Electromagnetic Systems" FIU Electronic Theses and Dissertations. 3514. https://digitalcommons.fiu.edu/etd/3514.

[49] **Sullivan, G. A., Blandino, J. R., Hayes, T. S., Jr., & Amato, T. (n.d.).** *Boom deployment mechanism for CubeSats*. Virginia Military Institute, Lexington, VA, USA.

[50] **Editorial Team, everything RF.** (2021). What is an Anechoic Chamber? Everything RF. https://www.everythingrf.com/community/what-is-an-anechoic-chamber.

CURRICULUM VITAE

Name Surname : Rümeysa ÜSTÜNCAN

EDUCATION :

- **B.Sc.** : 2020, Ozyegin University (OzU), Faculty of Architecture and Design, Industrial Design, Istanbul Türkiye
- Erasmus Exchange Student: Universita degli Studi della Campania Luigi Vanvitelli Naples, Italy - Hyrid Design Lab

PROFESSIONAL EXPERIENCE

- Istanbul Technical University - Spacecraft Systems Design and Test Laboratory (USTTL) 2022-Present
- AirCar Corp. 2023
- Freelence Designer 2021-Present
- Soleilsky 2020-2021

REWARDS:

- Ozu Makeathon 2018 Jury Special Prize
- Citta della Scienza 2019

PUBLICATIONS, PRESENTATIONS AND PATENTS ON THE THESIS:

- **Rümeysa Üstüncan,** 2025: Design of an Origami Structured Deployable S-band Helical Antenna for 6U CubeSats, 4rd International Graduate Research Symposium, IGRS’25 May 13, 2025 Istanbul, Türkiye